

FUNCTIONAL IMPACT OF NATURAL ORGANIC MATTER ON THE  
ADSORPTION OF 2-METHYLISOBORNEOL AND GEOSMIN  
TO POWDERED ACTIVATED CARBON

by  
Micala Mitcek

A thesis submitted to the Faculty and Board of Trustees of the Colorado School of Mines  
in partial fulfillment of the requirements for degree of Master of Science (Environmental  
Engineering Science).

Golden, Colorado

Date \_\_\_\_\_

Signed: \_\_\_\_\_  
Micala Mitchek

Signed: \_\_\_\_\_  
Dr. Christopher Bellona  
Thesis Advisor

Golden, Colorado

Date \_\_\_\_\_

Signed: \_\_\_\_\_  
Dr. Junko Munakata Marr  
Department Head

## ABSTRACT

To remedy drinking water taste and odor outbreaks, municipalities commonly utilize powdered activated carbon (PAC) to reduce the concentration of the two of the most abundant odorants, 2-methylisoborneol (MIB) and geosmin (GSM), down to their low parts per trillion odor threshold limits. Natural organic matter (NOM), typically present at low parts per million concentrations, critically impedes PAC's ability to adsorb these odorants. In order to further elucidate the leading mechanism of NOM interference on MIB and GSM adsorption, batch testing of odorant removal by three PAC products was conducted in a variety of synthetic and natural surface water sources. An analysis of the PAC dosages required to remove MIB and GSM down to their odor threshold limits in various NOM sources showed that for most waters, PAC adsorption performance was dependent only on NOM concentration and not NOM character. Subsequently, a simplified version of the ideal adsorbed solution theory-equivalent background component (IAST-EBC) model was adapted to successfully predict removal performance given odorant and NOM initial concentrations for a range of NOM sources. Finally, a comparison of removal performance between three mesoporous PACs highlighted combined micropore and mesopore volume to be the key activated carbon property that leads to enhanced resilience to NOM competition.

## TABLE OF CONTENTS

ABSTRACT .....	iii
LIST OF FIGURES.....	vi
LIST OF TABLES .....	viii
LIST OF EQUATIONS .....	ix
LIST OF ABBREVIATIONS .....	x
ACKNOWLEDGMENTS.....	xi
CHAPTER 1 INTRODUCTION .....	1
1.1. Motivation .....	1
1.2. Background .....	2
1.2.1. Characterization of odorants 2-methylisoborneol (MIB) and geosmin (GSM) ...	2
1.2.2. Characterization of natural organic matter (NOM) .....	3
1.2.3. Occurrence of odorants and NOM in the environment .....	5
1.2.4. Treatment of MIB, GSM, and NOM in drinking water treatment plants.....	6
1.3. Research hypothesis .....	6
1.3.1. Hypothesis 1 - The adsorption performance of a particular powdered activated carbon (PAC) for MIB and GSM removal from most surface water sources is dependent on dissolved organic carbon (DOC) concentration and independent of NOM characteristics.....	7
1.3.2. Hypothesis 2 - A simplified predictive model based on DOC and MIB or GSM initial concentrations can be utilized to predict PAC adsorption performance for MIB and GSM from a variety of surface water sources. ....	7
1.3.3. Hypothesis 3 - PAC's physiochemical properties, including pore volume and surface functionalities can be engineered to improve resilience to competitive adsorption of DOC. ....	8
CHAPTER 2 LITERATURE REVIEW .....	9
2.1. Impact of background water quality on MIB and GSM adsorption to PAC .....	9
2.2. Impact of water treatment process conditions on MIB and GSM adsorption to PAC ...	11
2.3. Modeling competitive impact from NOM on trace component adsorption .....	13
2.4. Impact of PAC physiochemical properties on MIB and GSM adsorption .....	14
CHAPTER 3 MATERIALS AND METHODS .....	17
3.1. Reagents .....	17
3.2. Activated carbon products .....	17

3.3. Synthetic and natural water samples .....	18
3.4. Batch experiments .....	19
3.5. Analytical methods .....	19
CHAPTER 4 RESULTS AND DISCUSSION .....	21
4.1. PAC performance for MIB and GSM removal in the presence of NOM.....	21
4.2. Development of a predictive model .....	25
4.2.1. Model calibration and verification .....	27
4.2.2. Extracting fundamental parameters .....	28
4.3. Engineering PAC for improved resilience to NOM competition .....	30
CHAPTER 5 CONCLUSIONS AND RECOMMENDATIONS .....	36
REFERENCES CITED .....	38
APPENDIX A SUPPLEMENTARY PAC CHARACTERIZATION DATA .....	42
APPENDIX B ADDITIONAL WATER QUALITY INFORMATION .....	43
APPENDIX C FREUNDLICH ADSORPTION ISOTHERMS .....	44
APPENDIX D MIB AND GSM REMOVAL CURVES .....	51
APPENDIX E DOC REMOVAL CURVES .....	55

## LIST OF FIGURES

Figure 4.1	PAC dosage required to achieve approximate odor threshold limit for MIB (top - 75% removal from 60 ppt) and GSM (bottom – 90% removal from 60 ppt). Filled in data points represent individual removal curves for conforming waters (UM, Source A, Source B, and Source C at various initial DOC concentration described in Table 3.2). Other symbols represent non-conforming waters (square is SWR NOM, triangle is Source D, plus is SWR HW, star is SWR FA). Solid line is a polynomial line of best fit for conforming waters and dotted lines illustrate $\pm$ one standard deviation as determined from triplicate removal curves in the same water.....	22
Figure 4.2	Percent DOC removal from a starting concentration of $3.4 \pm 0.4$ ppm versus PAC dosage for three different water sources (triangle is source D, cross is source B, and circle is source A). Solid line is a line of best fit for all data and dotted lines illustrate plus or minus one experimental standard deviation....	24
Figure 4.3	Predicted versus experimental PAC dosage required to reach set relative removal for MIB (left) and GSM (right). Dotted lines represent $\pm 15\%$ error.....	28
Figure 4.4	Incremental pore volume in critical pore width ranges in $\text{cm}^3$ per gram for the PAC products evaluated.....	31
Figure 4.5	PAC dosage required to achieve approximate odor threshold limit for MIB (top - 75% removal from 60 ppt) and GSM (bottom – 90% removal from 60 ppt) as a function of DOC initial concentration in conforming waters (UM NOM, source A, source B, and source C waters for CP500 and source A water for CPH and CP800F).....	32
Figure 4.6	Total micropore plus mesopore volume (tPV) PAC required to achieve the odor threshold limit for MIB (top - 75% removal from 60 ppt) and GSM (bottom – 90% removal from 60 ppt) as a function of DOC concentration in conforming waters (UM NOM, source A, source B, and source C waters for CP500 and source A water for CPH and CP800F). Error bars are included for CPH and CP800F to represent plus or minus one standard deviation in experimental error.....	34
Figure A.1	Cumulative pore volume up to 500 angstroms in $\text{cm}^3$ per gram measured by nitrogen adsorption and modeled by density functional theory.....	38
Figure C.1	Non-equilibrium adsorption isotherms for MIB and GSM onto CP500 (top) CPH (middle) CP800F (bottom) in NOM-free waters. Units of $q_{\text{MIB}}$ and $q_{\text{GSM}}$ are in $\mu\text{g/g}$ and units of $C_{\text{MIB}}$ and $C_{\text{GSM}}$ are in $\text{ng/L}$ . Trend lines represent Freundlich lines of best fit.....	42
Figure C.2	Non-equilibrium adsorption isotherms for MIB onto CP500 in surface waters and synthetic waters. Units of $q_{\text{MIB}}$ are in $\mu\text{g/g}$ and units of $C_{\text{MIB}}$ and in $\text{ng/L}$ . Trend lines represent Freundlich lines of best fit.....	43

Figure C.3	Non-equilibrium adsorption isotherms for GSM onto CP500 in surface waters and synthetic waters. Units of $q_{GSM}$ are in $\mu\text{g/g}$ and units of $C_{GSM}$ and in $\text{ng/L}$ . Trend lines represent Freundlich lines of best fit.....	44
Figure C.4	Non-equilibrium adsorption isotherms for MIB onto CPH and CP800F source A and SWR NOM synthetic water at 3, 6, and 9 ppm DOC. Units of $q_{MIB}$ are in $\mu\text{g/g}$ and units of $C_{MIB}$ and in $\text{ng/L}$ . Trend lines represent Freundlich lines of best fit.....	45
Figure C.5	Non-equilibrium adsorption isotherms for GSM onto CPH and CP800F in source A and SWR NOM synthetic waters at 3, 6, and 9 ppm DOC. Units of $q_{GSM}$ are in $\mu\text{g/g}$ and units of $C_{GSM}$ and in $\text{ng/L}$ . Trend lines represent Freundlich lines of best fit.....	46
Figure D.1	MIB removal curves for CP500 conducted at 60 ppt MIB and 30-minute contact time in: SWR HA, SWR FA, SWR NOM, UM NOM, source A, source B, and source C.....	47
Figure D.2	GSM removal curves for CP500 conducted at 60 ppt GSM and 30-minute contact time in: SWR HA, SWR FA, SWR NOM, UM NOM, source A, source B, and source C.....	48
Figure D.3	MIB removal curves for CPH and CP800F conducted at 60 ppt MIB and 30-minute contact time for source A and SWR NOM at 3, 6, and 9 ppm DOC.....	49
Figure D.4	GSM removal curves for CPH and CP800F conducted at 60 ppt GSM and 30-minute contact time for source A and SWR NOM at 3, 6, and 9 ppm DOC.....	50
Figure E.1	DOC removal curves using CP500 in synthetic and source waters at various initial DOC concentrations.....	51
Figure E.2	DOC removal curves using CPH and CP800F in SWR NOM and Source A waters both at 6 ppm DOC initially.....	51

## LIST OF TABLES

Table 1.1	Chemical properties of MIB and GSM (Clercín, 2019) .....	3
Table 3.1	PAC product properties .....	18
Table 3.2	Characteristics and source of waters used .....	19
Table 4.1	Summary of parameters used to estimate the EBC fractional concentration.....	29
Table 4.2	Simplified IAST-EBC parameters derived from evaluation of CP500, CPH, and CP800F in conforming waters.....	35
Table A.1	Temperature programmed desorption of surface oxygen functional groups from carbon surface. Water desorbed at room temperature originates from external moisture while that desorbing at higher temperature originates from internal or chemisorbed moisture. CO <sub>2</sub> primarily originates from carboxylic acid groups while CO originates primarily from phenolic hydroxyl groups or quinone carbonyl functionalities .....	38
Table B.1	Summary of inorganic content of Source A and B waters as determined by Inductively Coupled Mass Spectroscopy.....	39
Table C.1	CP500 Freundlich parameters for MIB and GSM adsorption determined in NOM-free water, synthetic waters, and source waters.....	40
Table C.2	Freundlich parameters for MIB and GSM adsorption to CPH determined in NOM-free water, SWR NOM, and source A waters.....	41
Table C.3	Freundlich parameters for MIB and GSM adsorption to CP800F determined in NOM-free water, SWR NOM, and source A waters.....	41



## LIST OF EQUATIONS

Equation 4.1	$C_1 = \frac{q_1}{q_1+q_e} \left( \frac{n_1 q_1 + n_e q_e}{n_1 k_1} \right)^{n_1}$ .....	25
Equation 4.2	$C_e = \frac{q_e}{q_1+q_e} \left( \frac{n_1 q_1 + n_e q_e}{n_e k_e} \right)^{n_e}$ .....	25
Equation 4.3	$q_1 = C_1 q_e^{1-n_1} \left( \frac{k_1 n_1}{n_e} \right)^{n_1}$ .....	26
Equation 4.4	$q_e = K_e C_e^{\frac{1}{n_e}}$ .....	26
Equation 4.5	$C_C = \frac{n_e}{n_1 k_1} C_{e,0}^{1-\frac{1}{n_1}} \left( \frac{C_{1,0}}{C_1} - 1 \right)^{\frac{1}{n_1}}$ .....	26
Equation 4.6	$\ln \left( \frac{C_{1,0}}{C_1} - 1 \right) = n_1 \ln(C_C) - B$ .....	27
Equation 4.7	$B = n_1 \ln \left( A(DOC)^{1-\frac{1}{n_1}} \right)$ .....	27
Equation 4.8	$A = \frac{n_e}{n_1 k_1} \left( f \frac{10^6 C}{MW_{NOM}} \right)^{1-\frac{1}{n_1}}$ .....	27

## LIST OF ABBREVIATIONS

MIB	2-methylisoborneol
GSM	geosmin
NOM	natural organic matter
TOC	total organic carbon
DOC	dissolved organic carbon
NPOC	non-purgeable organic carbon
SUVA	specific ultraviolet absorbance
IHSS	International Humic Substances Society
TGA	temperature programmed desorption
IAST	ideal adsorbed solution theory
EBC	equivalent background component
DFT	density functional theory
CP500	CarbPure <sup>®</sup> 500 PAC
CPH	CarbPure <sup>®</sup> H PAC
CP800F	CarbPure <sup>®</sup> 800F PAC
MCL	maximum contaminant level
ppt	parts per trillion
ppm	parts per million
PAC	powdered activated carbon
GAC	granular activated carbon
tPV	total micropore and mesopore volume

## ACKNOWLEDGMENTS

I would like to acknowledge many people and organizations who have helped me to succeed in completing this dissertation. First, I would like to thank my advisor, Dr. Chris Bellona, for providing me with the opportunity to experience research in an academic setting and for helping me to grow as a professional in environmental engineering. I would also like to thank the Bellona research group for their helpful discussions and my committee members for their time and advice: Dr. Timothy Strathmann, Dr. Joe Wong, and Dr. Chris Bellona.

Second, I would like to thank Advanced Emission Solutions, Inc. (ADES), and specifically my manager Dr. Joe Wong, for giving me the opportunity to pursue higher education while maintaining my employment and for supporting and encouraging me through the process. ADES graciously allowed me to utilize laboratory resources to gather data in support of completing this thesis. In addition to Joe, I would like to thank my colleagues for their collaboration and assistance: Ariel Li, David Park, Lingyan Song, Cesar Garcia, and Taren Leighton.

Finally, I would like to thank my family, especially my partner, Ben Metropulos, and my parents, Dan and Bonnie Mitchek, for their unending love and reassurance.

## CHAPTER 1

### INTRODUCTION

#### 1.1. Motivation

In addition to meeting primary drinking water maximum contaminant levels (MCLs), meeting aesthetic water quality standards (i.e., secondary standards) is critical when delivering drinking water to communities. While controlling taste, odor, and color of drinking water is not deemed vital for eliminating risk to human health and the environment, these factors are essential in achieving a positive public perception of water quality. For this reason, the US Environmental Protection Agency has established non-enforceable limitations on the aesthetic quality of water under National Secondary Drinking Water Regulations and it is a priority of public water works to control the aesthetic quality of the water they supply (US EPA, 2021).

Two of the most common constituents responsible for taste and odor episodes are 2-methylisoborneol (MIB) and geosmin (GSM). It is estimated that somewhere between one fourth to one half of all municipalities in the US at least periodically experience MIB and GSM episodes (Rangel-Mendez and Cannon, 2005). While the odorants are not toxic, humans can detect them down to low parts per trillion (ppt or ng/L) concentrations. These extremely low odor threshold limits challenge removal by conventional water treatment methods and drive requirements for targeted treatment. Perhaps the most commonly utilized treatment technology is powdered activated carbon (PAC) because of its operational flexibility and low capital cost. According to a 1996 American Water Works Association survey, PAC was available to about 48 percent of surface water systems with the primary purpose of use for odor control (Edzwald, 2012).

PAC's performance in controlling taste and odor outbreaks from surface water treatment plants is highly variable both geographically and seasonally. Performance discrepancies may originate from differences in the background water quality, differences in the water treatment process steps and conditions, and/or differences in the PAC's physiochemical properties. Of particular importance is interference from natural organic material (NOM) because it is present at parts per million (ppm or mg/L) levels in surface waters making it 30,000 to 300,000 times more abundant than the odorants of interest. The aim of this research is to further elucidate the leading mechanism of NOM interference on MIB and GSM adsorption onto activated carbon,

apply a fundamental adsorption model to predict removal performance, and to quantify activated carbon properties that lead to enhanced resilience to NOM competition.

## **1.2. Background**

To provide background for this research, information is provided to characterize both the odorants of interest and NOM. Additionally, a description of their occurrence in the environment and fate in drinking plants is provided.

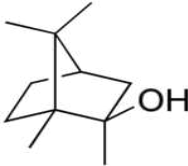
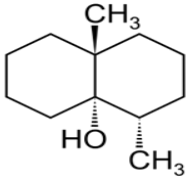
### **1.2.1. Characterization of odorants, MIB and GSM**

In addition to MIB and GSM, there is a long list of microbially derived odorants. These molecules are often secondary metabolites used by organisms primarily for the purpose of communication. These chemicals are used to deliver messages between individual organisms of the same species or even between different species and serve as info-chemicals at the ecosystem level. Additionally, these chemicals can act as attractants or as deterrents that modify the cellular functions of organisms (Liato and Aider, 2017).

Two of these chemicals, MIB and GSM, are responsible for the vast majority of taste and odor outbreaks in drinking water sources. The fact that the smell of rain is generally attributed to one of these chemicals, GSM, highlights their abundance in the environment (Yuhas, 2012). Compared to other odorants, MIB and GSM are extremely stable in the environment, are resistant to degradation through conventional water treatment methods, and have extremely low odor threshold limits (Watson et al. 2008). GSM has a characteristically earthy aroma and can typically be detected by humans down to 4 ppt while MIB with its characteristically musty smell can typically be detected down to 15 ppt (Rangel-Mendez and Cannon, 2005).

Table 1.1 summarizes some important chemical properties of MIB and GSM. Both MIB and GSM are categorized as tertiary alcohols and contain aliphatic alcohol groups with very limited acidity (i.e., negligible acid-base properties). MIB is a small tent shaped molecule with a molecular weight of 168 grams per gmole that is moderately hydrophobic, non-ionizable and volatile. GSM has similar properties, but is slightly larger at 182 grams per gmole, and has a longer, flatter shape consisting of two six-membered rings connected on one side. Both molecules are chiral and are only biologically produced as the negative enantiomers (Watson et al. 2008).

Table 1.1 Chemical properties of MIB and GSM (Clercín, 2019)

Property	MIB	GSM
Molecular structure		
Molecular formula	C <sub>11</sub> H <sub>20</sub> O	C <sub>12</sub> H <sub>22</sub> O
Odor	Musty	Earthy
Odor threshold conc. ppt	15	4
Molecular weight (g/gmol)	168.3	182.3
logK <sub>ow</sub>	3.12	3.7
Aqueous solubility (mg/L, 25°C)	194	150
Boiling point, (°C)	196	165
Density (g/cm <sup>3</sup> )	0.93	0.95
Vapor pressure (Pa, 25°C)	6.68	5.49
Henry's law constant (Pa m <sup>3</sup> /gmol)	5.76	6.66

### 1.2.2. Characterization of NOM

Natural organic matter (NOM) plays an important role in the chemistry of water systems. NOM is composed of a diverse range of organic chemicals with various structures making characterization challenging. NOM includes any synthetic organic chemicals that might be present, but their concentration is typically sufficiently low as to generally be considered negligible. Thus, NOM is primarily derived from natural processes, which might include decomposition of plant or aquatic biomass (Brezonik, 2011). The source can be autochthonous, meaning that its production occurs within the water body, or allochthonous, meaning it is formed elsewhere before being transferred to the body of water of interest (Edzwald, 2012). Additionally, the functional term, dissolved organic material (DOM), is often used to describe the portion of the NOM that passes through a 0.45µm filter (Brezonik, 2011). The terms total organic carbon (TOC) and dissolved organic carbon (DOC) refer to NOM and DOM on a carbon basis.

NOM is often categorized as being either hydrophilic or hydrophobic. In this description, carbohydrates and peptides are considered to be hydrophilic and humic material is considered hydrophobic. These designations are used lightly as many of these compounds contain both hydrophilic and hydrophobic functionalities and can behave differently depending on the characteristics of the source water (Brezonik, 2011). At low pH values, the acid components of

the humic substances are protonated making the molecules relatively hydrophobic. However, this hydrophobicity is not sufficient to allow them to repel water, and at higher pH values, the humic substances can be hydrophilic (Brezonik, 2011).

The hydrophilic or non-humic matter can include biological macromolecules such as proteins and polysaccharides and other plant by-products and metabolites. Compared to humic materials, this fraction is generally lower in molecular weight, more aliphatic, more autochthonous in origin, less effectively removed by coagulation/clarification/filtration treatment processes, and more easily broken down by natural processes (Edzwald, 2012).

In contrast, humic materials are rarely characterized by their individual structures. Instead, humic matter, which is often the dominant organic component of terrestrial aquatic systems, can be further categorized into humic acid, fulvic acid and humin based on solubility (IHSS, 2020). The hydrophobicity and solubility characteristics used here are defined operationally. There are many ways to fractionate and extract NOM, but for this study the definitions used by the International Humic Substances Society (IHSS) are used as they are some of the most widely applied methods. The hydrophilic fraction of NOM is defined by not having adsorption affinity for a hydrophobic ion exchange resin (XAD-8). The NOM fraction that adsorbs onto the hydrophobic resin and precipitates at a pH of one is considered humic acid, the portion that is soluble under all pH conditions is considered fulvic acid, and the fraction that is insoluble under all pH conditions is humin (IHSS, 2020).

These designations cannot uniformly be correlated to the structure or properties of humic materials, since the inhomogeneity of their sources makes them functionally diverse and recalcitrant with a large range in molecular weights. Some generalizations can be made though. Humic and fulvic acids are inhomogeneous mixtures of organic acids. Single extractions can yield thousands of unique chemical compounds. Typically, fulvic acid makes up the majority of the NOM mass in terrestrial water systems. Compared to humic acids, fulvic acids generally have lower molecular weights (averaging less than 1,000 compared to around a few thousand grams per gmole), are more highly charged, less aromatic, lower in nitrogen content, less retained in soils and more hydrophilic (Brezonik, 2011; Edzwald, 2012). Humic and fulvic acids generally have similar carbon, hydrogen and oxygen content with acidic carboxyl and phenol-OH groups. The deprotonation of these groups, particularly carboxyl groups, means that humic matter usually carries a negative charge in natural waters (Brezonik, 2011).

### **1.2.3. Occurrence of odorants and NOM in the environment**

Taste and odor episodes are experienced, at least periodically, by somewhere between one fourth to one half of all municipalities in temperate or tropical climates (Rangel-Mendez and Cannon, 2005). When MIB and GSM turn up in drinking water sources, cyanobacterial blooms are often considered to be the culprit. Warm climates and sufficient nutrient loading lead to increased microbial production. Predicting the occurrence of taste and odor episodes is difficult because even between closely related microbial taxa, the production capacity of taste and odor compounds varies significantly (Watson et al., 2016). While some odorants and other secondary metabolites are excreted continuously throughout the cell's lifecycle, MIB and GSM are primarily retained inside cells and not commonly released during the growth phase of the microbial growth cycle; instead, bulk releases occur during the death phase (Watson et al., 2016). The intermittent release of taste and odor causing chemicals can be explained through the complex lifecycle of some of the main MIB and GSM producing microbes which are generally filamentous and spore forming (Jüttner and Watson, 2007). This results in a type of slug excretion which causes more severe odor episodes as the chemicals are released in waves instead of continuously (Watson et al., 2008).

In a typical cycle, MIB and GSM concentrations spike to around 50 to 150 ppt for about a month. This spike often occurs in the summer and is concurrent with algal blooms. The concentrations will fall to around 10 to 30 ppt for the following several months then reach near zero levels for the remainder of the year (Rangel-Mendez and Cannon, 2005).

Similarly, although maybe less drastically, NOM varies seasonally and regionally. While odorants are typically present at ppt levels, NOM is present at ppm levels. TOC concentrations in groundwaters are typically less than 2 ppm, while in surface waters concentrations can range from 1 to 30 ppm with typical values of 5 ppm or less (Edzwald, 2012). The higher end concentrations usually originate in eutrophic lakes or streams and rivers that are fed by swamps, bogs, or marshes (Edzwald, 2012). Since NOM and taste and odor compounds are both derived from biological activity in surface waters, high levels of NOM in waters often challenge taste and odor control.



#### **1.2.4. Treatment of MIB, GSM, and NOM in drinking water treatment plants**

Without the addition of PAC, typical conventional water treatment processes are incapable of economically removing MIB and GSM. Neither coagulation or common oxidants (chlorine and potassium permanganate) can be economically optimized for MIB and GSM removal. Some advanced oxidation technologies (ozone and UV with hydrogen peroxide) have been proven capable of destroying MIB and GSM but are cost-prohibitive because of high dosage requirements (Srinivasan and Sorial, 2011). Similarly, understanding of the few biological treatment mechanisms that have been identified is limited (Srinivasan and Sorial, 2011). MIB and GSM's general stability throughout conventional water treatment as well as the seasonal nature of taste and odor outbreaks makes PAC the most practical and economical treatment technology available. PAC is most commonly added at low ppm levels as a slurry to the rapid mixer, but it can also be added during flocculation or sedimentation treatment steps. A typical contact time for PAC may be 30 minutes or no more than two hours from the rapid mix step to sedimentation or filtration steps when PAC is removed (Rangel-Mendez and Cannon, 2005). Where other, non-seasonal contaminants are also targeted for removal, continuous treatment with granular activated carbon (GAC) is a practical alternative (Edzwald, 2012).

Adsorption is also used in some cases to target NOM reductions because NOM can cause color and form hazardous disinfection byproducts during chlorination. When NOM is targeted for adsorption with PAC, the purpose is often to meet requirements of the Disinfectants-Disinfection Byproducts Rule which requires between 15 and 50 percent TOC removal depending on the source water TOC level and alkalinity (US EPA, 2021). Significant NOM reduction often requires similar to higher PAC dosages than what is required to remove MIB and GSM. Even when NOM is not a target constituent and PAC is used for the sole purpose of removing odorants, NOM will compete with odorants for PAC adsorption sites and pose challenges to effective removal of MIB and GSM.

#### **1.3. Research Hypotheses**

The overall objective of this research is to apply a fundamental and mechanistic evaluation of source water and activated carbon properties and features to quantify the impact of competitive adsorption by NOM on the capacity and selectivity of PAC for adsorbing MIB and GSM.

**1.3.1. Hypothesis 1 - The adsorption performance of a particular PAC for MIB and GSM removal from most surface water sources is dependent on DOC concentration and independent of NOM characteristics.**

Although a number of authors have studied the influence of NOM characteristics on the ability of PAC to adsorb MIB and GSM, most have focused on differentiating the impacts of various NOM fractions. In these cases, surrogate molecules are used to represent competition from a particular type of NOM compound or NOM is partitioned into fractions (based on hydrophobicity, charge, and/or molecular size) prior to performing MIB and GSM adsorption tests. Where the impact of non-fractionated NOM has been studied, samples have generally been limited to water from a discrete geography. This research aims to confirm that variations in the competitive impact between unique NOM fractions is much larger than variations in the competitive impact between whole water (non-fractionated) NOMs even if the whole water NOMs originate from diverse geographical regions. It is proposed that the competitive impact of NOM can be explained primarily through differences in the DOC concentration. As such, a set of synthetic waters was created to compare the competitive impact of NOM from the most common NOM fractions (humic and fulvic acids) to the competitive impact of whole water NOM from diverse regions. An advantage of using synthetically produced waters is the ability to reproduce the water characteristics for subsequent studies. Surface water samples from diverse regions of the US were also collected to be compared with the whole water NOM standard water sources. For these experiments, one PAC product was used.

**1.2.2. Hypothesis 2 - A simplified predictive model can predict PAC adsorption performance for MIB and GSM from most surface water sources.**

Through testing of the first hypothesis, it can be postulated that only the initial concentrations of DOC and the odorant of interest are necessary to estimate dosage requirements for the specific PAC of interest to achieve a specified odorant removal goal. As such, a simplified competitive adsorption model which has previously been used to predict PAC performance in a specific natural water source at any trace contaminant initial concentration was identified and adapted to include DOC initial concentration as an independent variable.

**1.2.3. Hypothesis 3 - PAC's physiochemical properties, including pore volume and surface functionalities, can be engineered to improve resilience to competitive adsorption by NOM.**

The predictive model developed in the above section was used as a research tool to examine the mechanisms of competitive adsorption. Learnings were applied to guide selection of PAC products with pore volume distributions that were predicted to enhance PAC's resilience to NOM competition. The impact of NOM on two additional PACs with unique pore volume distributions and surface chemistries was evaluated.

## CHAPTER 2

### LITERATURE REVIEW

#### **2.1. Impact of background water quality on MIB and GSM adsorption to PAC**

NOM is generally present in surface waters at concentrations five to six orders of magnitude higher than MIB and GSM. It follows that the adsorption capacity of different PACs for MIB and GSM removal decreases, often up to ten times, when NOM is introduced (Bandosz, 2006; Newcombe et al. 2002b; Graham et al. 2000).

There are two leading mechanisms that attribute to the effects of competitive adsorption: direct competition and pore blocking (Hepplewhite et al. 2004; Rescorla et al. 2017; Bandosz, 2006; Matsui et al. 2013; Li et al., 2003). During direct competition, the competing molecule, usually containing similar physical and chemical properties to the constituent of interest, has an affinity for the same adsorption sites. The two molecules compete to fill adsorption sites and effectively decrease the adsorption capacity available to each component. A more diverse set of competing molecules can contribute to the second mechanism, pore blocking. In this case, molecules that are larger than the constituent of interest can be adsorbed in wider pores subsequently blocking access to the smaller pores which sequester the target molecule. Where the target and the competing constituent are exposed to PAC simultaneously, as in a batch system, the relatively slower diffusion of the larger competing compound would limit the impact of pore blocking (Shimabuku et al., Newcombe et al. 2002b). Still, pore blocking by small molecular weight compounds is possible.

Li et al. isolated these two mechanisms by observing the impact of two model competitive compounds on trace organic (atrazine) adsorption. The model compound with similar molecular weight to the target exemplified direct competition by decreasing equilibrium adsorption capacity by approximately 75 percent. Pore blocking was exemplified when very minimal decreases in equilibrium capacity were observed for a microporous PAC in the presence of the large molecular weight (18,000 g per gmole) model competing compound while no changes were observed for a PAC containing micropores and mesopores. Micropores are defined by the International Union of Pure and Applied Chemistry as pores with a width of less than 20 angstroms, while mesopores are defined as pore widths between 20 and 500 angstroms. Li et al. showed that kinetics of the trace compound's adsorption were only impacted when the large

molecular weight compound was pre-loaded onto the PAC. Hence, the major mechanism impacting trace contaminant adsorption in the presence of NOM is direct competition via NOM molecules with similar molecular weight to the target component.

Newcombe et al. expanded this understanding by using an array of six diverse PACs and six NOM fractions separated by size, polarity, and concentration. They concluded that bulk water parameters alone, such as DOC adsorption, were not sufficient to explain the competitive effect of NOM on MIB adsorption. Instead, small molecular weight NOM with similar size and structure to MIB contributed most significantly to competition. As the molecular size cutoff of the NOM fractions decreased, the competitive effect increased, but the largest impact was observed for raw water. The raw sample probably contains many of the smallest NOM fractions that are likely to be lost during fractionation. It follows that direct competition is the leading mechanism at play (Newcombe et al. 2002b). Matsui et al. also highlighted direct competition via very-low molecular weight chromophoric NOM as the primary competing mechanism for MIB and GSM using a wood-based PAC and three types of water samples (Matsui et al. 2012, Matsui et al. 2013).

The work conducted by Newcombe et al, helped to explain competitive adsorption mechanisms by showing that different fractions of NOM impose different magnitudes of competition. While this was important in helping to explain underlying mechanisms, it is highly unlikely that NOM characteristics would vary so significantly between water sources. Even though NOM constitutes a highly heterogeneous mixture of unique compounds, the structural, chemical, and physical properties of NOM from distinct sources are generally reasonably consistent (Brezoik et al 2011). As such, it is reasonable to assume that the competitive impact caused by NOM may not vary significantly from site to site. Following this hypothesis, Newcombe and Cook attempted to correlate easy-to-measure water characteristics to PAC performance. They showed that the percent MIB and GSM remaining correlated to DOC level, and UV254 absorbance within the same water source (diluted and sampled at different times). When percent MIB and GSM remaining was plotted versus DOC level for a range of waters these correlations failed ( $R^2$  values between 0.1 and 0.54 were achieved). Water source information for the wide range of waters was not given. The authors concluded that water quality parameters can be used to predict PAC performance in one water source but not broadly. They did suggest that the compilation of a database with MIB removal, DOC, and UV254 absorbance

might be able to predict PAC performance at least in semi-quantitative manner (Newcombe and Cook, 2002).

While NOM might be the most important background water quality metric determining PAC performance in removal of odorants, it can still be important to consider other water quality parameters. These include pH, alkalinity, and ionic strength. Newcombe and Cook explored the influence of alkalinity and ionic strength on MIB and GSM removal and concluded no impact within typical environmental conditions (Newcombe and Cook, 2002). MIB and GSM are generally unaffected by pH as they are nonionizable at conditions relevant for drinking water treatment. It follows that their adsorption onto PAC is not affected by pH (Bandosz, 2006; Graham et al. 2000; Newcombe and Cook, 2002). On the other hand, humic materials are more protonated and more hydrophobic at lower pH values. Thus, in NOM impacted waters, decreasing pH has been shown to increase competitive adsorption hindering the removal of taste and odor compounds by PAC (Bandosz, 2006; Graham et al. 2000). This has been quantified to a 6 percent decrease in sorption capacity for a decrease in one pH unit using ten source waters and a microporous PAC. There is also an effect of ionic strength on NOM character in which divalent cations can interact with NOM and decrease their size (Edzwald, 2012). No known study has observed a difference in NOM competition from changes to the ionic strength of the background water.

## **2.2. Impact of water treatment process conditions on MIB and GSM adsorption to PAC**

Water treatment process parameters and the sequence in the treatment process where PAC is dosed play a significant role in determining PAC adsorption performance. Particular factors of importance are contact time as well as PAC dosing in relation to coagulation or oxidation treatment steps.

The adsorption rates of taste and odor compounds vary with PAC properties at time scales relevant to a typical drinking water treatment plant operation. Newcombe et al., showed that equilibrium was reached somewhere between 60 and 240 minutes for six PACs made from a range of source materials and activation methods. Because of this, performance ranking at 30 minutes is significantly different than performance ranking at two hours. Carbons with a more mesoporous structure and with higher total pore volume generally show quicker adsorption kinetics. Other studies similarly show superior performance of mesoporous lignite-based PACs compared to more microporous bituminous-based PACs at short contact times (Bandosz, 2006).

This effect is often attributed to a more open pore volume distribution increasing the accessibility of adsorption sites (Hepplewhite et al. 2004).

Conflicting results have been generated regarding the influence of coagulation on the performance of PAC. It has been hypothesized that coagulation will effectively make PAC particles less dispersed by encapsulating the PAC in flocs. This could cause kinetic disadvantages and block pore entrances. At moderate coagulant doses though (less than around 40 ppm), studies have generally shown no effect of coagulates on odorant adsorption (Bandosz 2006, He et al. 2016; Rescola et al. 2017). One such study showed that PAC performance was very similar in water both pre- and post-flocculation (Zoschke et al. 2011). Zoschke et al. suggested that flocculation is selective for the opposite NOM fractions compared to those which are important for competitive adsorption. That is, the smaller NOM fractions that are responsible for competitive adsorption are relatively unaffected by coagulation. On the other hand, larger NOM fractions are most prominently impacted by flocculation and generally insignificant for competitive adsorption.

In other cases, though, the presence of coagulants during adsorption has shown mixed impact on performance. Mailler et al. showed that injection of ferric chloride slightly improved the uptake of a number of micropollutants. They suggested that the removal of the colloidal NOM fraction effectively decreased the extent of competitive adsorption onto PAC. A decrease in performance in the presence of coagulation was seen in a number of other studies (Newcombe and Cook, 2002; Shimabuku et al. 2014; Seckler et al. 2013). This decrease has been hypothesized to result from decreasing pH which increased NOM competitive adsorption as well as limited access to adsorption sites due to incorporation of PAC particles into flocs. If odorant adsorption occurs upstream of coagulation, it is possible for NOM to displace the odorant as the pH decreases during coagulation (Bandosz, 2006). Seckler et al. showed a 15 percent decrease in MIB removal in the presence of coagulants. The incorporation of PAC to the floc was visible which suggests that the metal hydroxide precipitates may have formed within the PAC particles and PAC particles themselves were bound to flocs causing an increase in mass transfer resistance from the bulk liquid and within the PAC's internal pore structure. The dosing point for PAC pre- or post-coagulation though was irrelevant as long as a sufficient hydraulic residence and mixing time was available for sorption.

The inconsistencies at play in studying the impact of coagulation on PAC adsorption highlight the multi-faceted nature of the process. Coagulants affect many properties that have the potential for changing adsorption dynamics and different operating conditions likely cause different mechanism to control performance. Contact time, injection location, PAC adsorption kinetics, pH swings, or concentration and fraction of NOM present could each play a decisive role in determining PAC performance.

Oxidants (chlorine, chloramines, permanganate, ozone etc.) have consistently shown negative impacts for the adsorption of hydrophobic contaminants to PAC. Oxidation can transform NOM in ways that increase competitive adsorption by causing a downward shift in the molecular weight distribution or producing chlorinated disinfection by-products that have a higher affinity for PAC than the original NOM (Newcombe and Cook, 2002). Additionally, oxidants can react with the PAC surface to form oxygen functional groups. These functional groups on the PAC's surface can act to decrease the hydrophobicity of the adsorbent and/or restrict access to pores through steric hinderance. This effect was shown by He et al. where PAC performance increased when the lag time between pre-chlorination and PAC dosing was increased (He et al. 2016).

### **2.3. Modeling NOM's competitive impact on trace component adsorption**

There are a number of models that have been used to describe competitive adsorption. One of the most common is the ideal adsorbed solution theory (IAST) which is based on a thermodynamic description of direct competition. The IAST describes the adsorption of a mixture when single-component adsorption parameters of the individual compounds in the mixture are known. A challenge arises when attempting to model NOM in this way because of its heterogeneous nature. This problem can be overcome by assuming that a single equivalent background component (EBC) can describe the total decrease in adsorption of the target contaminant. In this way, the competitive impact of trace component in NOM containing water has been successfully modeled by a number of authors (Graham et al., Newcombe and Cook 2002, Matsui et al. 2012, Matsui et al. 2013, Shimabuku et al. 2014, Edzwald 2012).

Graham et al showed that, for three of four natural waters tested, the competitive effect of NOM on MIB and GSM could be described by an initial concentration of the EBC that made up only 0.45 molar percent of the water's initial DOC. For the fourth water, which was identified as industrially impacted, the percent of DOC that made up the EBC was three times that amount.



Matsui et al. similarly found the competing fraction of NOM to account for a small percentage of the total (less than 2 percent). They correlated this fraction of NOM to low molecular weight (less than 230 grams per gmol) chromophoric NOM (Matsui et al. 2012, Matsui et al. 2013). Shimabuku et al. found a single model that was able to predict MIB removal from eight unique non-wastewater impacted source waters using the IAST-EBC with the initial concentration of the EBC equal to 0.51 molar percent of the total initial DOC. The proportion of competitive NOM in two wastewater impacted sources of surface water was significantly higher (Shimabuku et al. 2014).

#### **2.4. Impact of PAC characteristics on MIB and GSM adsorption**

A number of studies have concluded that even though not all carbons perform the same for removal of MIB and GSM there is no one surrogate carbon parameter (surface area, total pore volume, methylene blue number, iodine number etc.) that can predict performance (Tennant and Mazyck, 2007; Hepplewhite et al. 2004; Newcombe et al. 2002; McCallum et al. 2002; Yu et al. 2007; Jaman et al, 2019; Edzwald, 2012). The raw material source used in producing PAC also does not predict carbon performance, because the same carbon properties can be produced from a variety of starting materials by modifying activation conditions (Shimabuku et al. 2014; Bandosz, 2006; Jamen et al. 2019; Newcombe et al. 2002). Surrogate parameters such as iodine number or BET surface area often correlate well when the solid-phase concentration of the constituent of interest is high, such as in solvent recovery applications, but removal of trace components is not as straight forward. One likely reason for this lack of correlation is because the initial concentrations of the trace constituents are far below their solubility limit where adsorption would be maximized (Edzwald, 2012). Instead, trace component adsorption occurs primarily in high energy adsorption sites where pore dimensions closely resemble target adsorbate dimensions (Edzwald, 2012).

Although neither surrogate parameters nor carbon source alone are suitable indicators of performance, it is clear that pore volume and pore volume distribution play an important role in facilitating adsorption. For natural waters, a bimodal pore volume distribution with sufficient micropore and mesopore volume has been deemed desirable because it is very difficult to design a carbon with pores specific for MIB or GSM when the primary component driving NOM competition is molecules of similar size and structure to the target (Hepplewhite et al. 2014). A number of studies have attempted to correlate a specific pore volume range to MIB and GSM

performance, but the recommended pore widths vary from study to study depending on background water conditions and the particular PACs evaluated. For example, this critical pore width has been reported to be 5.4 to 63 angstroms (Nowack et al., 2004), 12 to 100 angstroms (Tennant and Mazyck, 2007), 10 to 12 angstroms (Heppelwhite et al. 2004), or 7 to 10 angstroms (Newcombe et al. 2002), or 5.4 to 400 (Rangel-Mendez and Cannon, 2005). It is clear that pore volume is critical for odorant adsorption, but inconsistencies from various studies suggest that different mechanisms limit adsorption in different systems. The study by Rangel-Mendes highlights the effect of carbon type on defining the critical pore volume since the specific pore volume range that correlated to performance between lignite-based GAC variations falls apart with the addition of a bituminous-based GAC. They also illustrated that the upper bound on the critical pore volume is vague (either 63 to 400 angstroms) and suggest that this results from the impact of competitive adsorption. Additionally, pore geometry (pore conformation in either layers, slits, or holes etc.) may impact adsorption kinetics and capacity (Marsh and Rodriguez-Reinoso, 2006).

The role of carbon surface chemistry in driving adsorption has also been debated. Activated carbon surface hydrophilicity and charge are generally attributed to acidic oxygen functional groups. These functional groups can increase water adsorption and aid in the formation of water clusters at pore edges (McCallum et al. 2002; Tennant and Mazyck, 2007). The adsorbed water hinders pore accessibility and the functional groups themselves can be agents of steric hinderance. Rangel-Mendez demonstrated an ability to improve MIB adsorption by increasing carbon surface hydrophobicity via steam and methane and steam treatment of lignite based GACs. The impact of surface hydrophobicity could not be isolated though because slight changes in pore volume were also observed. Moreover, the effect of PAC surface chemistry is not consistent over variable testing conditions and background water qualities. Tennant and Mazyck showed that increasing the concentration of acidic functional groups on bituminous-based carbons with similar physical characteristics negatively impacted MIB adsorption in DI water, but that this detrimental effect decreased as the background TOC concentration increased until the effect was negligible in raw surface water.

It is clearly seen from past literature that no single carbon feature drives performance. Instead, performance is likely driven by a limiting mechanism (e.g., pore volume distribution or surface chemistry) which is specific to the carbon of interest and the system it is being used in.

This study aims to investigate particular carbon features that are most important in controlling PAC adsorption performance under various background water quality conditions.

## CHAPTER 3

### MATERIALS AND METHODS

This chapter describes the experimental design for performing batch testing to explore the competitive adsorption impacts of NOM on MIB and GSM. Described are the materials used, methods performed, and analytical procedures.

#### **1.1. Reagents**

A combined certified reference standard of concentrated (100  $\mu\text{g/mL}$ ) MIB and GSM and sodium bicarbonate were purchased from Sigma Aldrich (St Louis, MO). Standard NOM reference compounds for preparation of synthetic water samples were purchased from the International Humic Substances Society (IHSS, Ames, IA). These standards including Suwannee River III HA, Suwannee River III FA, Suwannee River NOM, and Upper Mississippi River NOM were received as dry powders. Instant ocean was purchased from PetSmart (Phoenix, AZ) because it contains all the major and minor inorganic constituents at ratios representative of the natural environment. Deionized water containing less than 0.3 ppm TOC was generated by reverse osmosis (GE Osmotics, Minnetonka, Minn.) for preparation of synthetic waters and for dilution of source waters. HPLC grade water (Sigma Aldrich St Louis, MO) was used for preparation of an ultra-clean NOM-free source water.

#### **3.1.1. Activated carbon products**

Activated carbon samples were obtained from CarbPure Technologies LLC, a subsidiary of Advanced Emissions Solutions, Inc. The first stage of experiments which examines difference in NOM type and source on carbon performance utilized CarbPure<sup>®</sup> 500 (CP500). CP500 is a steam activated lignite-based PAC which was selected because it is widely used by municipalities to combat taste and odor episodes. During the second stage of testing CarbPure<sup>®</sup> H (CPH) and CarbPure<sup>®</sup> 800F (CP800F) were included. PAC product properties are described in Table 3.1 All PAC products have equivalent D50 particle sizes implying essentially equivalent external surface area to volume ratios of 0.25. The biggest change in carbon properties seen when moving from a baseline of CP500 to CPH is an increased pore volume, particularly in the mesopore (20 - 500 Å) range. A further increase in pore volume (both mesopores and micropores) is seen when moving to CP800F, but this change is accompanied by changes to additional carbon features, most significantly a doubling of the surface oxygen functional group

content as measured by temperature programmed desorption coupled with a mass spectrometer analysis.

Table 3.1 PAC product properties

Property	Unit	CP500	CPH	CP800F
Iodine number	mg/g	542	573	800
pH	-	11.1	11.0	7.3
D50 particle size	µm	24.0	23.7	23.4
Tapped density	g/mL	0.47	0.41	0.34
Moisture	wt%	1.9	1.9	3.4
Volatiles	wt%	5.8	5.0	8.7
Ash	wt%	24.0	26.0	15.4
Fixed carbon	wt%	68.4	67.1	72.4
Micropore volume (<20 Å)	cm <sup>3</sup> /g	0.20	0.18	0.31
Mesopore volume (20 - 500 Å)	cm <sup>3</sup> /g	0.30	0.43	0.64
Micropore/mesopore volume	-	0.66	0.42	0.49
Pore volume up to 500Å	cm <sup>3</sup> /g	0.50	0.62	0.95
Total oxygen functional groups	wt%	3.0	3.3	5.9

### 3.1.2. Synthetic and natural water samples

Natural water samples were collected from several municipalities around the US. Each of these municipalities is known to experience regular taste and odor episodes and utilize PAC for mitigation. Two natural water sources were diluted to achieve a range of DOC concentrations listed in Table 3.1 (Source A and B). Deionized dilution water was spiked with the appropriate concentrations of inorganic salts to match major cation and anion concentrations as measured by inductively coupled plasma mass spectrometry (Table B.1).

Synthetic waters were generated by spiking deionized water with 350 ppm of instant ocean sea salt to achieve a typical surface water level of total dissolved solids, 50 ppm of sodium carbonate buffer and the appropriate level of IHSS NOM to achieve the desired DOC concentration. If necessary, pH was adjusted to adjusted to  $7.2 \pm 0.2$  with NaOH or HCl. Two types of standard NOMs were used: reverse osmosis isolates, referred to as whole water NOMs, which incorporate all fractions of NOM present in a natural water source and isolates of humic and fulvic acids. Table 3.2 outlines characteristics of all natural and synthetic water sources used in this study.

Table 3.2 Characteristics and source of waters used.

Water Abbreviation	Water Source Location	Water Source Type	DOC levels tested (ppm)	pH	SUVA (Lm/mg)
SWR	Suwannee River	IHSS	3, 6, 9 ± 0.3	7.2±0.2	3.4
	NOM	standard			
UM	Upper Mississippi	IHSS	3, 6, 9 ± 0.3	7.2±0.2	3.8
	NOM	standard			
SWR HA	Suwannee River	IHSS	3, 6, 9 ± 0.3	7.2±0.2	6.7
	Humic Acid	standard			
SWR FA	Suwannee River	IHSS	3, 6, 9 ± 0.3	7.2±0.2	4.8
	Fulvic Acid	standard			
Source A	Southeast	River	3.3, 6.3, 9.3, 12.2	7.4	3.3
Source B	Midwest	River	2.1, 3.6, 5.0, 6.3	7.8	1.9
Source C	Midwest	Lake	3.9	7.8	2.3
Source D	Southeast	Reservoir	3.1	6.9	3.4

### 3.1.3. Batch experiments

Adsorption experiments were conducted in 50 milliliter flasks using rubber stoppers to prevent volatilization. MIB and GSM were spiked to achieve a nominal concentration of 60 ppt. Control samples were included during every experiment to quantify any losses. A micropipette was used to dose PAC from a concentrated slurry into each microcosm. A 30-minute contact time was chosen to mimic feasible exposure at a typical drinking water treatment plant. Jars were stirred on a stir plate at 150 revolutions per minute at room temperature before being vacuum filtered to separate out the PAC. Pre-rinsed 0.7-micron glass fiber filter paper (Pall Corporation, Port Washington, NY) was used for DOC analysis while 0.45-micron GN-6 Metrical (Pall Corporation) filter paper was used for MIB and GMS analysis.

### 3.1.4. Analytical methods

MIB and GSM were measured by headspace-solid phase microextraction-gas chromatography/mass spectrometry (Agilent 7000D GC/TQ). DOC was measured with a Shimadzu (Kyoto, Japan) Total Organic Carbon Analyzer using the non-purgeable organic carbon (NPOC) method. UV254 was measured with a Beckman Coulter (Brea, CA) DU 800 spectrophotometer and SUVA was calculated as the UV254 absorption divided by the DOC. All analyses were run as duplicates.

Bulk composition of PAC products was conducted by thermogravimetric analysis (TGA) via ASTM methods D2866-94 for ash, D2867-09 for moisture, and D5832-98 for volatile matter

and fixed carbon content was calculated by difference. PAC particle size distribution was measured by a Micromeritics Saturn DigiSizer II (Atlanta, GA) employing high resolution laser light scattering. Tapped density was measured by ADSM D8176-18, pH was measured by ASTM D3838-05, and iodine number was measured by ADSM D4608-14. Pore volume distribution data were achieved through applying a density functional theory (DFT) model to nitrogen adsorption data performed in a Micromeritics 3Flex surface characterization analyzer. Analysis of the surface oxygen functional group content of the PAC products was conducted at Western Kentucky University's Thermal Analysis Laboratory utilizing a TA Q600 SDT (New Castle, DE) interfaced using a heated capillary transfer pan to a Pfeiffer Thermostar mass spectrometer (Aßlar, Germany). Approximately 20 milligrams of sample were held at room temperature for 30 minutes then heated to 900°C at 10°C per minute under an argon atmosphere. Then, temperature dependent weight loss was quantified by TGA and off-gas was qualified by mass spectroscopy (Thermal Analysis Laboratory, 2021).

## CHAPTER 4

### RESULTS AND DISCUSSION

#### 4.1. PAC performance for MIB and GSM removal in the presence of NOM

Removal curves were generated to quantify differences in MIB and GSM adsorption onto CP500 in the 22 various natural water and synthetic water sources that were summarized in Table 3.2. Individual removal curves can be found in Appendix D. Waters tested included well-characterized whole water NOMs and NOM fraction standards as well as surface waters from diverse regions in the US. To compare performance across water sources, a PAC dose required to reach the odor threshold limit was plotted against DOC concentration in Figure 4.1 on page 22. At the same DOC concentration, an increase in the required PAC dose indicates an increase in NOM competition. Similar to what is utilized at water treatment plants, PAC dosages in the range of 10 to 100 ppm were necessary. Consistent with past literature, GSM is more easily adsorbed than MIB. For both odorants, there is a clear influence of increasing DOC concentration resulting in an increased required PAC dosage across all water types. As DOC concentration increases there is a diminishing increase in the competitive impact as seen by the decreasing slope in the trend line on Figure 4.1.

With the exception of source D and SWR NOM, the whole water NOMs all follow a consistent trend in the operational competitive effect observed as a function of DOC concentration. For these conforming waters 87 and 93 percent of removal curves fell within the experimental standard deviation for MIB and GSM, respectively. This was true even as the waters varied in surface water type (lakes versus rivers), source location (midwestern US versus southeastern US), NOM-type (isolated versus collected), and SUVA (3.4 to 1.9 L/mg-M). Even though NOM constitutes a highly heterogeneous mixture of unique compounds, the structural, chemical, and physical properties of NOM from distinct sources are usually reasonably consistent (Brezonik et al., 2011). As such, it appears that for most water sources, differences in NOM character are not large enough to cause differences in their associated competitive effect.



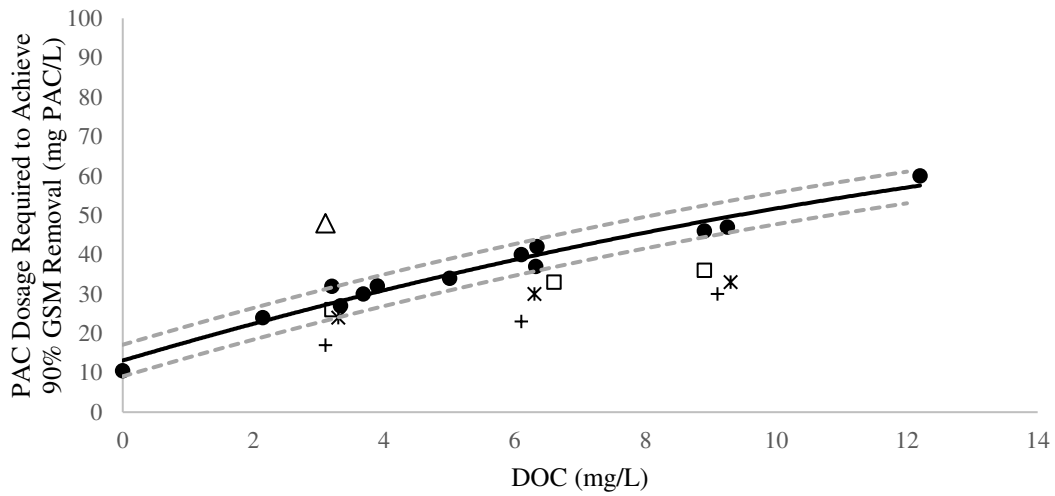
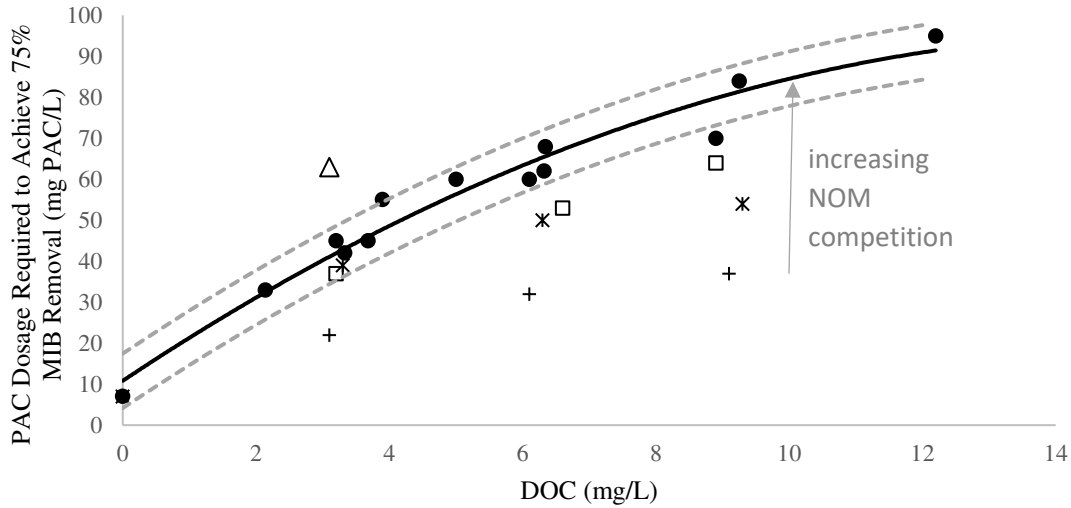


Figure 4.1 PAC dosage required to achieve approximate odor threshold limit for MIB (top - 75% removal from 60 ppt) and GSM (bottom – 90% removal from 60 ppt). Filled in data points represent individual removal curves for conforming waters (UM, Source A, Source B, and Source C at the various initial DOC concentration described in Table 3.2). Other symbols represent non-conforming waters (square is SWR NOM, triangle is Source D, plus is SWR HW, star is SWR FA). Solid line is a polynomial line of best fit for conforming waters and dotted lines illustrate  $\pm$  one standard deviation as determined from triplicate removal curves in the same water.

SWR NOM was isolated by the IHSS from the Okefenokee Swamp specifically because the water contains up to 100 ppm DOC with very minimal cations and impact from human activity (IHSS, 2020). UM NOM was later isolated from the Mississippi River to better represent NOM from a typical surface water (IHSS, 2020). The slightly shallower competitive impact trend observed for SWR NOM may be due to these unique characteristics. Regardless, a

comparison of SWR NOM to SWR FA and SWR HA is useful to discern which fraction of NOM exhibits the highest competitive impact. A decreasing trend in the competitive impact is seen when moving from the SWR NOM to SWR FA to SWR HA (Figure 4.1). Humic matter (primarily humic and fulvic acids) typically makes up the majority of NOM compounds in surface waters (Brezonik, 2006). During the separation procedure used by the IHSS, 12 and 48 weight percent of the total NOM were reportedly isolated as humic and fulvic acid, respectively (IHSS, 2020). As an example, in a water containing 6 ppm of DOC as SWR NOM, this would equate to 0.7 ppm of DOC as SWR HA and 2.9 ppm of DOC as SWR FA. An attempt was made to compare performance at these equivalent SWR HA and SWR FA concentrations. At 6 ppm DOC as SWR NOM, about a 650 and a 210 percent increase in PAC dosage compared to NOM-free water was required to achieve the odor threshold limit for MIB and GSM, respectively. Slightly less than 10 percent of this increase can be explained by the equivalent 0.7 ppm of DOC as SWR HA and slightly more than 50 percent of this increase can be explained by the equivalent 2.9 ppm of DOC as SWR FA for both odorants. From this analysis, it might be inferred that the majority of the competitive impact is caused by the humic NOM fraction (about 60 percent), but that the non-humic fraction of NOM is also responsible for a significant portion (about 40 percent) of the competitive impact. It should be noted, though, that the multistage process required to isolate the humic material standards could result in losses that might be biased towards small molecular weight hydrophobic NOM molecules. These same molecules would be expected to contribute most significantly to competitive adsorption and so it is likely that greater than 60 percent of the competitive impact was caused by humic materials.

The largest outlier in the similarity of the competitive impact of whole water NOMs was observed for source D. An attempt was made to use standard water characterizations to differentiate this NOM from other sources. The pH and SUVA values fell within the same range as the conforming waters so differences in acidity and NOM hydrophobicity were ruled out. NOM absorbability to CP500, as shown in Figure 4.2, was also found to be consistent between source waters A, B, and D all at similar initial DOC concentrations. Data confirming the lack of influence from changes in NOM source on the quantity of DOC adsorbed for two additional PAC products in source A and SWR NOM waters can be found in Appendix E. This agrees with previous work indicating that bulk NOM adsorption characteristics are not sufficient to explain the associated competitive effect (Newcombe et al. 2002b, Matsui et al. 2012 and 2013). This is

likely because the major contributing mechanism is direct competition by small molecular weight NOM that makes up only a small fraction of the total NOM present (Li et al., 2003; Newcombe et al., 2002b; Matsui et al., 2012 and 2013).

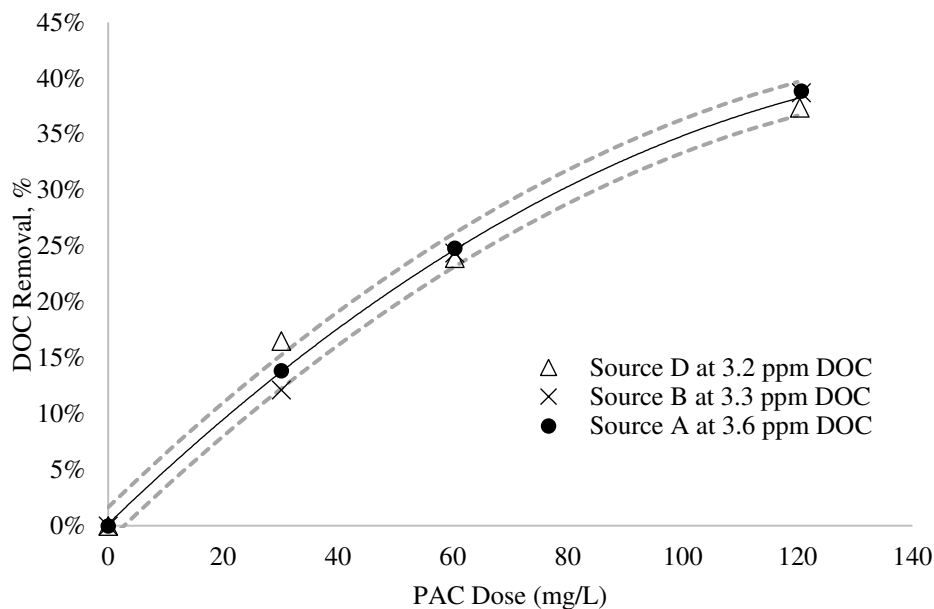


Figure 4.2 Percent DOC removal from a starting concentration of  $3.4 \pm 0.4$  ppm versus PAC dosage for three different water sources (triangle is source D, cross is source B, and circle is source A). Solid line is a polynomial line of best fit for all data and dotted lines illustrate plus or minus one experimental standard deviation.

While no quantitative characterizations were found that could differentiate source D from the conforming waters, the fact that it is the only reservoir water source tested might be an indication of the source's increased impact from human activity. Summers et al. found that wastewater impacted sources showed significantly higher competitive effects when compared to non-wastewater impacted sources. A single IAST-EBC model could be used to predict performance in eight non-wastewater impacted waters, but performance within wastewater impacted water sources did not follow a similar trend. It was hypothesized that the increased competitiveness of the source D water was caused by a small fraction of the NOM that originates from wastewater treatment discharge or other anthropogenic sources.

Freundlich parameters were determined for MIB and GSM in each of the NOM containing waters and NOM-free water (Table C.1). The Freundlich exponent ( $n$ ) is indicative of adsorption intensity or adsorption-site heterogeneity whereas the Freundlich coefficient ( $K$ ) is indicative of adsorption capacity or the number of adsorption-sites available (Pelekani and

Snoeyink, 1998). Across water types, increasing DOC concentration corresponded to a decreasing trend in the magnitude of  $K$ , while the variability in  $n$  does not follow any consistent trend. This supports the assumption that direct site competition is the primary mechanism for which NOM interacts with trace odorants.

These results support the hypothesis that adsorption performance of a particular PAC for MIB and GSM removal from most surface water sources is dependent on DOC concentration and independent of NOM characteristics. This conclusion does not exclude outliers; a more in-depth attempt at mapping the competitive impact of different water sources and determining the specific character of DOM that leads to the observed differences in competition would be helpful but is not the focus of this study. Instead, the general similarity in the observed competitive impact for the majority of waters was used as a pre-condition for building a predictive model. The predictive model can be used both as a tool for predicting PAC requirements under various DOC conditions and as a research tool aimed at better understanding the mechanism of NOM competition.

#### 4.2 Development of a predictive model

Based on the general similarity in adsorption behavior versus DOC concentration, a predictive model was used to relate the PAC dosage required to relative removal of MIB or GSM given initial concentrations of the odorant and DOC. This relationship was built by applying a non-equilibrium simplified version of the IAST-EBC model. The IAST-EBC model can be used to model the impact of NOM competition on trace component adsorption (Graham et al., 2000; Newcombe and Cook, 2002; Matsui et al., 2012 and 2013; Zoschke et al., 2011; Shimabuku et al., 2014). The latter two references proved the applicability of the IAST-EBC under non-equilibrium conditions with the limitation that parameters developed are only applicable at the specified contact time. Since NOM is composed of a diverse array of chemicals whose competitive impact and independent adsorption isotherms cannot be isolated, the EBC is used to represent a single component whose adsorption can account for the entire decrease in adsorption of the target component observed using the following equations:

$$C_1 = \frac{q_1}{q_1 + q_e} \left( \frac{n_1 q_1 + n_e q_e}{n_1 k_1} \right)^{n_1} \quad (4.1)$$

$$C_e = \frac{q_e}{q_1 + q_e} \left( \frac{n_1 q_1 + n_e q_e}{n_e k_e} \right)^{n_e} \quad (4.2)$$

Where  $C$  is the aqueous concentration at the contact time of interest,  $q$  is the solid-phase concentration, and  $K$  and  $\frac{1}{n}$  are single-component Freundlich parameters. The subscript 1 represents the trace component and subscript  $e$  represents the EBC. Parameters to describe the adsorption of the EBC can be extracted using the full version of the IAST-EBC model by conducting isotherms in natural water and back-solving for EBC initial concentration and Freundlich parameters. However, this approach is limited in its inability to determine a unique solution and its computational difficulty in requiring  $q_e$  to be approximated at every data point (Newcombe and Cook, 2002; Matsui et al., 2012 and 2013; Gillolgy et al., 1998; Qi et al., 2007). Instead, a simplification derived by Qi et al. was used in which Equations 4.1 and Equation 4.2 are first simplified by assuming that  $q_1 \ll q_e$  and that the Freundlich exponents are similar (between one and five).

$$q_1 = C_1 q_e^{1-n_1} \left( \frac{K_1 n_1}{n_e} \right)^{n_1} \quad (4.3)$$

$$q_e = K_e C_e^{\frac{1}{n_e}} \quad (4.4)$$

With these assumptions, the EBC equation becomes the single-component Freundlich isotherm meaning that when the solid phase concentration for the EBC is sufficiently high, its adsorption behavior is not dependent on the presence of the trace component. Conversely, the adsorption of the trace component is strongly dependent on the extent of adsorption of the competing component. Two additional simplifications were made by Qi et al. First, a pseudo single-solute isotherm equation is derived by assuming that the EBC initial concentration dominates the aqueous concentration  $\left( q_e = \frac{C_{e,0} - C_e}{C_c} \approx \frac{C_{e,0}}{C_c} \right)$ . Where  $C_{e,0}$  is the initial concentration of the equivalent background component and  $C_c$  is the carbon dose. The second simplification is made for the special case of a batch reactor (or a continuously stirred tank reactor with the substitution of fluxes for adsorbent mass and solution volume). Here, a mass balance around the target component  $(C_{1,0} = C_c q_1 + C_{1,0} q_1)$  can be used to relate the relative removal of the target component directly to carbon dose.

$$C_c = \frac{n_e}{n_1 K_1} C_{e,0}^{1-\frac{1}{n_1}} \left( \frac{C_{1,0}}{C_1} - 1 \right)^{\frac{1}{n_1}} \quad (4.5)$$

Equation 4.5 mathematically illustrates the phenomena of the independence of micropollutant initial concentration on percent removal that has been observed repeatedly for

micropollutants in the presence of NOM (Gilligly et al., 1998; Cook et al., 2001; Matsui et al., 2003). Mechanistically, an increase in initial micropollutant concentration garners it more competitive for adsorption sites increasing the extent to which it is adsorbed. Qi et al. used a linearized form of Equation 4.5 to isolate two well-defined model parameters. For the purpose of creating a global model to predict removal as a function of DOC concentration, the assumption that  $C_{e,0}$  accounts for a constant fraction of the total NOM were added here.

$$\ln\left(\frac{C_{1,0}}{C_1} - 1\right) = n_1 \ln(C_C) - B \quad (4.6)$$

With

$$B = n_1 \ln\left(A(DOC)^{1 - \frac{1}{n_1}}\right) \quad (4.7)$$

$$A = \frac{n_e}{n_1 K_1} \left(f \frac{10^6 C}{MW_{NOM}}\right)^{1 - \frac{1}{n_1}} \quad (4.8)$$

Where  $f$  is the mole fraction of  $C_{e,0}$  to the total initial molar concentration of NOM,  $MW_{NOM}$  is the molecular weight of NOM, and  $C$  is the weight fraction of carbon to total NOM. DOC is given in milligrams per liter and the  $10^6$  value is included in Equation 4.8 as a unit conversion assuming all other aqueous concentrations are in nanomolar units. The strength of this approach in its ability to quickly quantify two well defined parameters,  $n_1$  and  $A$  from a single removal curve in order to predict PAC performance at any initial target and background NOM concentration without the necessity of independently solving for  $C_{e,0}$  and  $n_e$ .

Alternatively, assumptions can be made for the uncertain parameters contained within  $A$  and  $f$ , which holds physical significance, can be used as the second fitting parameter. One limitation in using this approach arises from the thermodynamic derivation of the IAST which requires calculations to be made in molar quantities, whereas DOC, which is measured in milligrams per liter, represents a multi-component system of compounds with a range of molecular weights. The use of  $f$  as the second fitting parameter also adds the requirement of obtaining the single-solute Freundlich  $K_1$  for the PAC of interest. Only the linearized form of the IAST-EBC model was used here since the similarity of the linearized model with the full IAST-EBC has been confirmed by several authors (Qi et al., 2007; Zoschke et al., 2011).

#### 4.2.1 Model calibration and verification

Parameters  $n_1$  and  $B$  were determined using Equation 4.7 for five different DOC levels utilizing one synthetic water (UM NOM at 3, 6, and 9 ppm DOC) and two natural waters (source

A as received and at three dilution levels and source B as received and at one dilution level). Consistent  $n_1$  values were found for both MIB ( $1.6 \pm 0.2$ ) and GSM ( $2.1 \pm 0.07$ ) as this value represents the characteristic single-solute Freundlich exponent for the adsorbent and adsorbate. An average value for  $n_1$  was used in each case. The parameter A, which incorporates  $n_1, n_e, K_1, MW_{DOC}$ , and  $f$  into a single term, was then determined using MS Excel Solver by minimization of the sum of the squared errors between the data and the model outputs.

The model was then verified using batch testing data in as-received source C water and source B water at two additional dilution levels. Figure 4.3 shows predicted versus experimental required PAC dosages. Data was well modeled achieving R squared values of 0.99 for GSM and 0.97 for MIB.

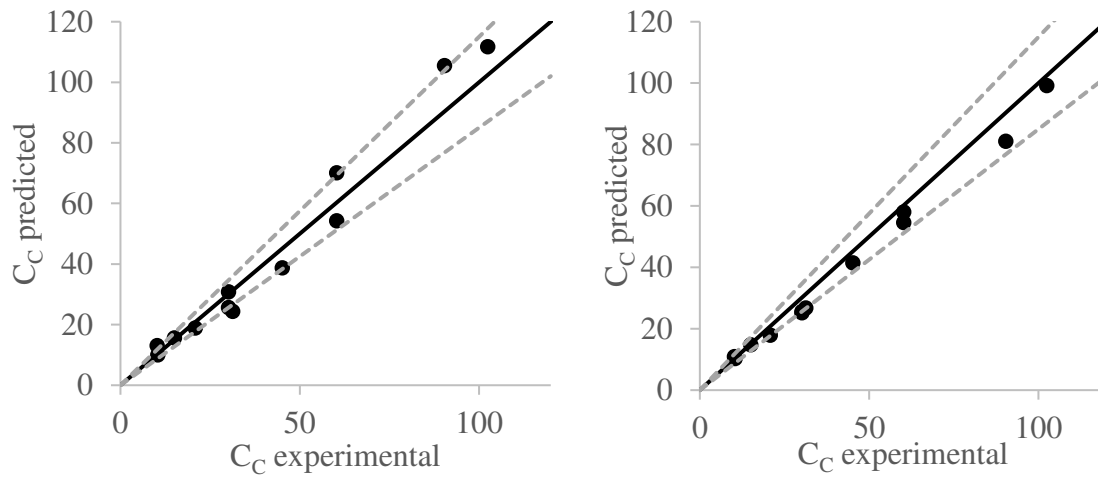


Figure 4.3 Predicted versus experimental PAC dosage required to reach set relative removal for MIB (left) and GSM (right). Dotted lines represent  $\pm 15\%$  error.

These results confirm the second hypothesis of this study by successfully predicting MIB and GSM removal from natural water sources that contain any initial odorant and DOC concentration. It should be noted that the particular parameters developed are characteristic to the specific PAC and contact time chosen. The strength of this approach is that it can be used quickly to calibrate model parameters for any particular PAC or contact time. At minimum, only one removal curve would be required to characterize  $n_1$  and the second parameter (A or  $f$ ) for any PAC/odorant pair.

#### 4.2.2. Extracting Fundamental Parameters

When using deionized water (which contains on average 0.3 ppm DOC) to perform NOM-free removal curves, repeatability was not sufficient for providing reliable results. To

remedy the analytical inconsistencies, the background water was changed to high-purity HPLC water and the PAC dosage required to achieve the odor threshold limit dropped from between 11 and 26 and between 12 and 22 ppm to 7 and 9 ppm for MIB and GSM, respectively. DOC measured in HPLC water was assumed to be negligible since results were below the instrument calibration limit. The fact that this seemingly small amount of DOC present in deionized water equates to 10,000 times the mass of the odorant can help explain the difference. A similar observation was made by Gillolgy et al. who postulated that even in NOM-free water, MIB and GSM do not portray a competitive impact on each other because the inevitably larger mass of NOM that is present dominates competition. This analysis can help explain why the  $n_1$  value determined from the simplified IAST-EBC model does not match the single-solute Freundlich exponent determined from adsorption in NOM-free water. For this reason, the  $n_1$  value determined from the simplified IAST-EBC was used for further analysis.

For the purpose of gleaning a fundamental understanding of the magnitude of the fraction of NOM that competes, assumptions (outlined in Table 4.1) were made for values contained within fitting parameter A. NOM was assumed to be 50 weight percent carbon and a range of average NOM molecular weights was used (IHSS, 2020). As a best guess, the EBC was taken to have equivalent molecular weight and  $n_e$  as the target component. The range of K values used originates from an experimentally determined NOM-free single-solute Freundlich constant and a Freundlich constant fitted using the  $n_1$  value determined from the simplified IAST-EBC analysis.

Table 4.1 Summary of parameters used to estimate the EBC fractional concentration.

Parameter	MIB			GSM		
	low end	best guess	high end	low end	best guess	high end
$MW_{NOM}$ g/mol	1500	2000	2500	1500	2000	2500
$MW_{EBC}$ g/mol	150	168	300	150	182	300
$n_e$ -	1	1.59	5	1	2.10	5
$k_1$ (nmol/mg)(L/nmol) <sup><math>n_1</math></sup>	0.05	0.05	0.11	0.07	0.07	0.10
$f$ , molar nmol <sub>EBC</sub> /nmol <sub>NOM</sub>	0.001%	0.04%	1.78%	0.002%	0.01%	0.15%
$f$ , mass ng <sub>EBC</sub> / ng <sub>NOM</sub>	0.0001%	0.004%	0.18%	0.0002%	0.001%	0.02%

This analysis shows that assumptions used create variations in the fraction of NOM that competes that span a few orders of magnitude. Regardless, the EBC makes up a very small



fraction of the total NOM present while still representing a greater concentration than the target component. For example, at 6 ppm DOC, under the best guess assumptions, the EBC concentration would be 157 ppt for GSM and 440 ppt for MIB. Also noteworthy is that the fraction of NOM that competes with MIB is four times that fraction that competes with GSM. This difference could result from some of the same characteristics (lower hydrophobicity, round compared to flat molecular shape) making MIB both less adsorbable and less effective at competing with NOM for adsorption sites compared to GSM.

### **4.3. Engineering PAC for improved resilience to NOM competition**

Adsorption of trace organics is thought to occur primarily in high energy adsorption sites where pore width is one to two times the width of the target adsorbent molecule. At this distance intermolecular forces such as capillary adsorption and van der Waals forces can interact on the target adsorbent from both sides of the pore wall (Edzwald, 2012). This critical pore size is described here as sequestration pore volume. For MIB and GSM, a sequestration pore volume of 5.4 – 11 angstroms can be assumed. Sequestration pore volume for NOM, estimated to range from 8 to 88 angstroms, is more difficult to describe since NOM is composed of a diverse collection of individual compounds. Elemental composition data from the IHSS website as well as distribution of molecular weights were used to estimate NOM molecular size ranges (Brezonik, 2011). An elemental volume contribution method was used to estimate the molecular volumes of MIB, GSM and NOM (Zhao et al., 2003).

MIB, GSM, and NOM adsorption capacity at the specified performance goal as seen in Figure 4.1 was converted to a percentage of the available sequestration pore volume that is filled. This equates to approximately 0.002% for MIB and 0.003% for GSM in NOM-free water. When NOM is present, the percentage of sequestration pore volume filled drops by 60% to 90% depending on the DOC concentration (2 to 9 ppm). This drastic decrease illustrates that even though there is an excess of sequestration pores, NOM molecules still outcompete the odorants for the adsorption sites that they would have occupied in NOM-free water. It was hypothesized that, in addition to sufficient pore volume for sequestration, the presence of larger pores, estimated to be up to 10 times the width of the molecule of interest is also critical. These larger pores, here called transport pores, aide in funneling contaminants towards high energy adsorption sites and increase diffusion kinetics. They would also increase diversity of adsorption sites with

the intention of creating NOM adsorption sites that are unique from MIB and GSM adsorption sites.

MIB, GSM, and NOM sequestration and transport pore volumes of the three carbons tested are described in Figure 4.4. With similar volumes of sequestration pores, CPH offers a moderate increase in MIB and GSM transport pore volume and NOM transport and sequestration pore volumes. Pore volume is further increased in CP800F. Although offering twice as much pore volume in the odorant transport pore and NOM sequestration pore width ranges, the surface acidity of CP800F is also doubled (Table A.1).

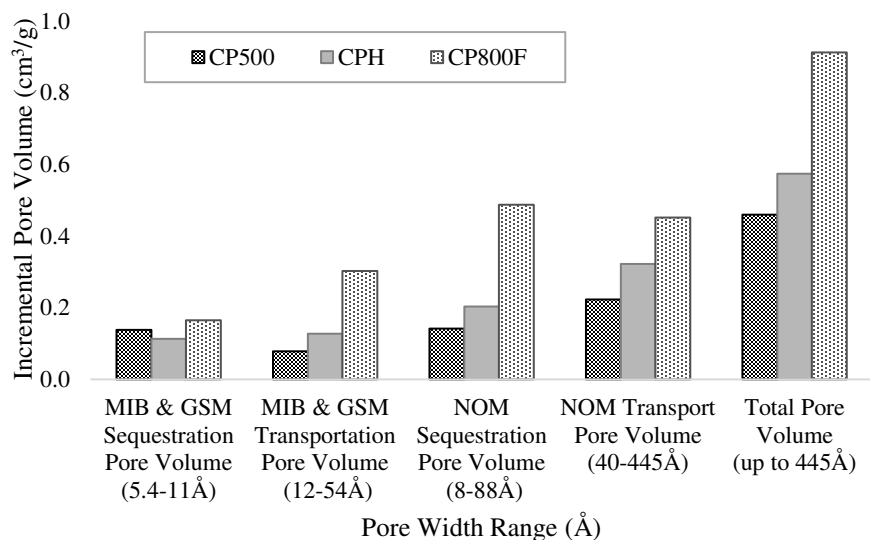


Figure 4.4 Incremental pore volume in critical pore width ranges in cm<sup>3</sup> per gram for the PAC products evaluated.

Under the same batch testing conditions used in the preceding sections, MIB, GSM, and DOC adsorption onto CPH and CP800F was evaluated. Removal curves were assessed in one synthetic water type (SWR NOM) and one surface water (Source A) each at DOC concentrations of 3, 6, and 9 ppm. Similar to what was seen for CP500, an increasing trend in competitive adsorption was observed as the DOC concentrations increased and a stronger impact was observed for source A water compared to SWR NOM. A full set of removal curves can be found in Appendix D and Freundlich isotherms can be found in Appendix C. For comparison, Figure 3.4 displays the PAC dosage required to achieve the MIB or GSM odor threshold limit as a function of initial DOC concentration for all three PACs in conforming waters (UM NOM, source A, source B, and source C waters for CP500 and source A water for CPH and CP800F).

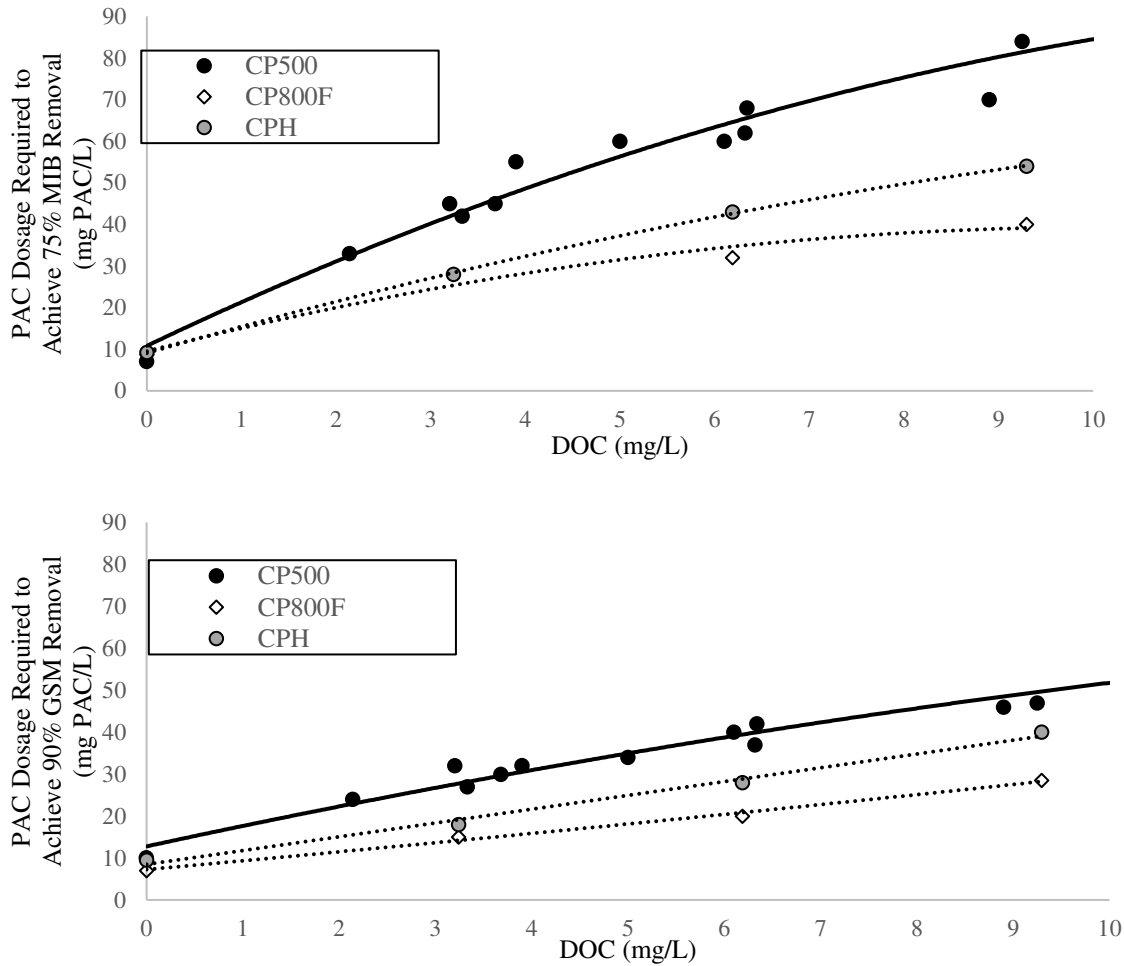


Figure 4.5 PAC dosage required to achieve approximate odor threshold limit for MIB (top - 75% removal from 60 ppt) and GSM (bottom – 90% removal from 60 ppt) as a function of DOC initial concentration in conforming waters (UM NOM, source A, source B, and source C waters for CP500 and source A water for CPH and CP800F).

Clearly, CPH and even more so CP800F require less PAC than CP500 to remove MIB and GSM at all DOC initial concentrations. While performance in NOM-free water follows the same trend, the differences were more exaggerated when NOM was present implying that the features incorporated into these carbons help to suppress the impact of competitive adsorption. CPH has very similar characteristics to CP500 with the exception of an increase in transport pores; specifically, CPH shows an increase in pores with widths greater than 30 angstroms (see pore volume distribution in Figure A.1). Depending on the DOC level used for evaluation, this 19% increase in pore volume accounted for an 18% to 33% decrease in the required PAC dosage to reduce both odorants to below their odor threshold limits. This is compared to a 10% decrease in PAC dosage in NOM-free water. The enhanced benefit of CPH over CP500 in NOM

containing water supports the hypothesis that increasing transport pore volume increases PAC's resilience to competitive adsorption. Functionally, the increase in larger pores is thought to create sites outside of the MIB and GSM sequestration pores where NOM can alternatively adsorb.

Similarly, the competitive advantage of CP800F increases in NOM containing water (from 15% to 30-50% and from 33% to 42-48% less CP800F is required compared to CP500 in NOM-free water compared to NOM containing water for MIB and GSM, respectively). Tracking carbon features responsible for these effects is less straight forward because of the multifaceted change in carbon properties, but it is likely that the significant increase in pore volume and in particularly transport pores plays a critical role.

To further clarify the impact of specific pore volume ranges on performance, PAC dosages from Figure 4.5 were converted from mg PAC per liter to cubic centimeters of pore volume per liter. The specific pore width range used to calculate the pore volume was adjusted until performance of the three carbons matched. When dosage was plotted on a total micropore plus mesopore volume basis (up to 500 angstroms), the performance for all three carbons coincides within experimental error (Figure 4.6). This correlation also held when the upper bound pore width cutoff was anywhere between 250 and 500 angstroms indicating that for these three PACs, performance is dependent on a combination of micropore and mesopore volume. This was true regardless of the differences in the relative ratio of micropores to mesopores (ranging from 0.42 to 0.66), and difference in surface acidity (ranging from 3.0 to 5.9 weight percent surface oxygen functional groups).

Total micropore plus mesopore volume may not describe PAC performance for all potential PAC products because all three carbons presented in this study are considered mesoporous carbons. The inclusion of a micropores PAC would help to clarify the necessity of both micropores and mesopores. It can be concluded that total pore volume up to 500 angstroms in mesoporous PACs should be maximized. Of course, as pore volume increases, so does the cost to manufacture the PAC product. A full cost analysis would be needed to determine which PAC performs best on a cost-performance basis. Intuitively, cost-performance at low background DOC concentrations may tend toward less expensive, lower pore volume PACs, while at high DOC concentrations, high pore volume mesoporous PACs may have the competitive advantage because of their relatively larger competitive advantage of at high DOC concentrations.

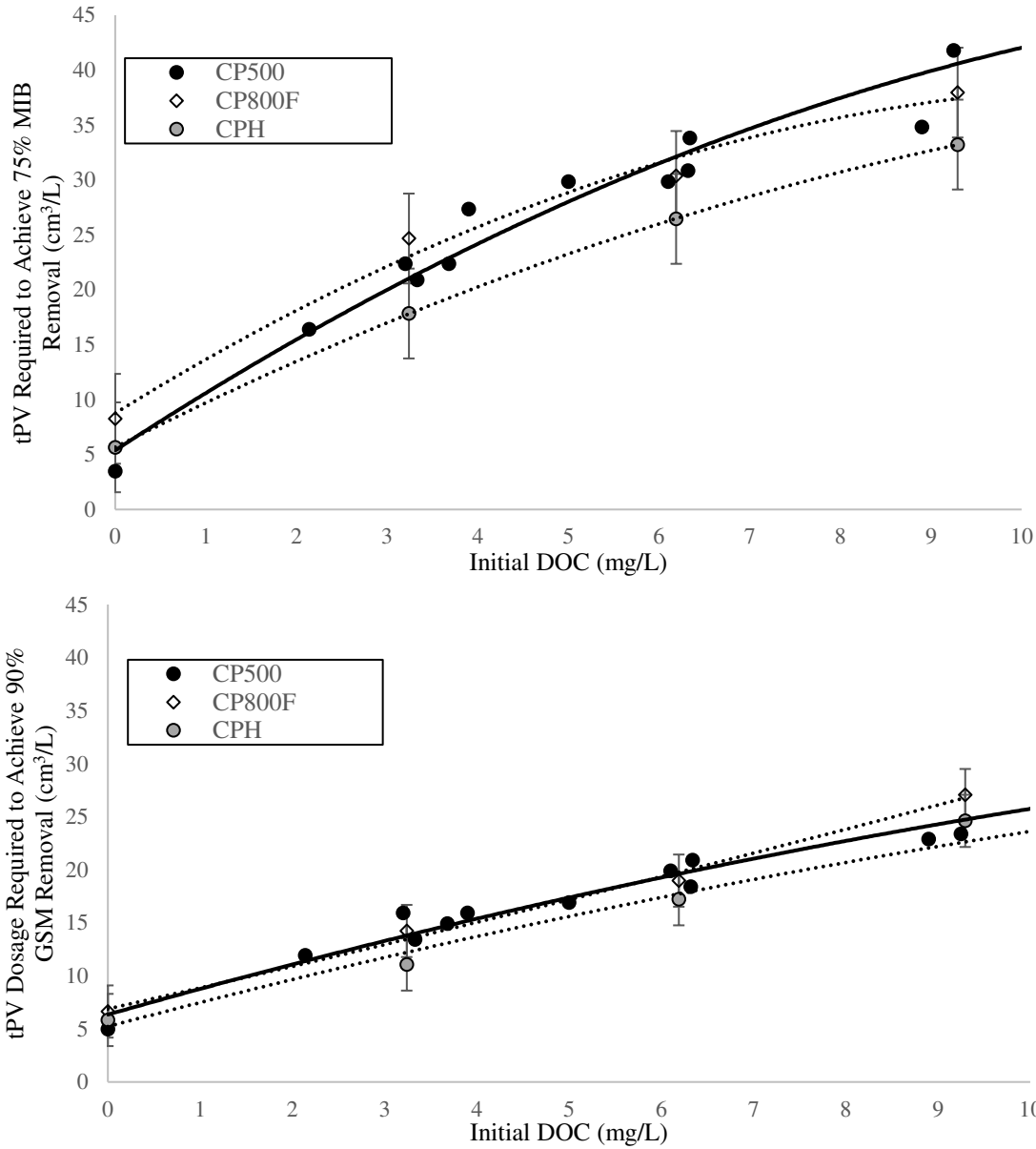


Figure 4.6 Total micropore plus mesopore volume (tPV) required to achieve the odor threshold limit for MIB (top - 75% removal from 60 ppt) and GSM (bottom - 90% removal from 60 ppt) as a function of DOC concentration in conforming waters (UM NOM, source A, source B, and source C waters for CP500 and source A water for CPH and CP800F). Error bars are included for CPH and CP800F to represent plus or minus one standard deviation in experimental error.

When comparing performance based on required PAC dosage, some of the functional information is lost. So, in an attempt to further elucidate the mechanisms driving differences in performance, the same simplified IAST-EBC analysis as discussed in Section 4.2.1 for CP500 was performed for CPH and CP800F in source A water. Best guess assumptions outlined in Table 4.1 were used and resulting parameters can be found in Table 4.2.

Table 4.2 Simplified IAST-EBC parameters derived from evaluation of CP500, CPH, and CP800F in conforming waters.

PAC	MIB			GSM		
	$K_1$	$n_1$	$f$	$K_1$	$n_1$	$f$
	(nmol/mg)* (L/nmol) <sup>n1</sup>	-	nmol <sub>EBC</sub> / nmol <sub>NOM</sub>	(nmol/mg)* (L/nmol) <sup>n1</sup>	-	nmol <sub>EBC</sub> / nmol <sub>NOM</sub>
CP500	0.052	1.59	0.044%	0.07	2.10	0.014%
CPH	0.067	1.52	0.032%	0.10	2.05	0.013%
CP800F	0.079	1.38	0.045%	0.16	1.73	0.020%

For both carbons, the increased performance was displayed more prominently in benefits to single-solute Freundlich parameters than in benefits to the percent of competing NOM as estimated by  $f$ . For CPH, a slight to moderate decrease in  $f$  was observed for both MIB and GSM, but for CP800F, there was actually an increase in the magnitude of  $f$  for both odorants. The increase in  $f$  observed for CP800F coinciding with lower competitive adsorption impacts is likely a result of the significant increase in pore volume or adsorption capacity. The increase in transport pores when moving from CPH to CP500 did give rise to an increase in the carbon's apparent non-equilibrium capacity in NOM-free water as observed through the increase in CPH's single-solute  $K_1$  value. This capacity increase observed under the non-equilibrium conditions used in this study was thought to originate from the advantage of increased diffusion kinetics resulting from transport pores improving access to adsorption sites because there is no improvement in adsorption pores. The further increase in single-solute  $K_1$  observed for CP800F is likely due both to improved diffusion kinetics and an increase in sequestration pore volume. The fact that performance differences are explained through multiple parameter changes demonstrates the multifaceted nature of PAC features that contribute to PAC performance.

The performance of CPH and CP800F in comparison to CP500 addressed the third hypothesis of this study which focused on the ability to engineer PAC's physiochemical properties to improve resilience to competitive adsorption. Indeed, increased total micropore and mesopore volume improved PAC performance across all DOC concentrations to a greater extent than in NOM-free water. It was concluded that the impacts of pore volume distribution outweigh the impacts of surface functionalities.

## CHAPTER 5

### CONCLUSIONS AND RECOMMENDATIONS

This study explored the impact of NOM on the adsorption of MIB and GSM to mesoporous PACs. It was concluded that: (1) for most surface waters, NOM character is sufficiently similar such that DOC concentration alone determines the magnitude of NOM's competitive impact on MIB and GSM adsorption, (2) a simplified IAST-EBC model can be adapted to predict the PAC dosage required to achieve a removal goal given NOM and odorant initial concentrations, (3) a very small fraction of NOM (less than 2 molar percent and less than 0.2 weight percent), as estimated from the modeled EBC initial concentration, accounts for NOM competition (4) for mesoporous carbons, resilience to competitive adsorption is built through maximizing a combination of micropore and mesopore volume, and (5) carbon surface character quantified through the concentration of surface oxygen functional groups up to 5.9 weight percent did not play a significant role in differentiating PAC performance.

The first conclusion was met through evaluation of MIB and GSM removal efficacy of CP500 being tested in a series synthetic and natural surface water sources at various DOC concentrations. Previous literature had suggested significant differences in NOM competition based on NOM type because NOMs were fractionated based on molecular size and/or polarity. This study quantified the significant difference in competitive effect of fractionated NOM compared to whole water NOMs. Alternatively, a majority of whole water NOMs from diverse sources exhibited similar impacts on MIB and GSM adsorption. This general similarity in the competitive impact of many different water types, ranging in source type (lakes versus rivers), source location (midwestern US versus southeastern US), NOM-type (isolated versus collected), and SUVA (3.4 to 1.9 L/mg-M) demonstrated that even though NOM constitutes a highly heterogeneous mixture of unique compounds, the structural, chemical, and physical properties of NOM from distinct sources are usually reasonably consistent and so the competitive impact of these different NOM types is also generally consistent.

The waters determined to have a similar competitive impact were then used to calibrate a model that predicted the dosages of PAC required to remove MIB or GSM for any DOC and odorant initial concentration. This modeling was done through adaption of a simplified non-equilibrium version of the IAST-EBC model. The calibrated model successfully predicted MIB

and GSM performance in two natural water sources with R squared values of 0.97 and 0.99, respectively. Parameters extracted from the model demonstrated that a very small fraction of the total NOM is responsible for the large competitive impact observed (less than 2 molar percent and less than 0.2 weight percent).

Finally, this study explored the functional impact of PAC features on determining carbon's resilience to NOM competition. It was hypothesized that larger, transport pores in addition to smaller, sequestration pores would aid in PAC's ability to adsorb competing NOM molecules without interfering with MIB and GSM adsorption. Indeed, enhanced performance both in NOM-free water and increasingly so in NOM-containing water was observed for two PACs which contained increased transport pore volume. When PAC performance was compared with respect to the PAC's total volume of combined micropore and mesopores dosed, all carbons performed the same, implying that performance is maximized when both micropore and mesopore volume is maximized. This was true for all three mesoporous carbon's regardless of significant differences in the PAC's surface functionalities.

One objective of future work would be to explore what caused certain water sources to be outliers in their competitive effect and to further clarify the characteristics of a water source that cause the competitive impact to deviate. One potential cause suggested in this work and also by Shimabuku et al., was the presence anthropogenic sources. Analysis for common indicators of anthropogenic sources might be used to expand the understanding of the water characteristics and types of source waters generate exceedingly challenging background conditions for adsorption of MIB, GSM and potentially other micropollutants.

An additional objective of future work would be to explore whether the same PAC properties identified in this study prove to be most critical for an expanded selection of PACs and an expanded selection of testing conditions. Particularly useful would be an investigation of the critical pore volume ranges driving performance when microporous PAC products are included as well as potential surface functionality impacts when the surface oxygen functional group content of the carbon surface exceeds 5.9 weight percent. Additionally, expanded analysis of PAC surface functionality and pore geometry/accessibility impacts is justified. Finally, with respect to testing conditions, a further analysis of contact time impacts is warranted. Especially useful would be an analysis of the impacts of changing carbon features on MIB and GSM adsorption and diffusion kinetics.



## REFERENCES CITED

- Bandosz, T. J. *Activated Carbon Surfaces in Environmental Remediation*; Interface science and technology ; v. 7; Elsevier: Amsterdam; 2006.
- Brezonik, P. L. *Water Chemistry: An Introduction to the Chemistry of Natural and Engineered Aquatic Systems*; Oxford University Press: New York, New York, 2011.
- Clercín, N. A. Origin and Fate of Odorous Metabolites, 2-Methylisoborneol and Geosmin, in a Eutrophic Reservoir. Ph.D., Indiana University - Purdue University Indianapolis, United States -- Indiana, 2019.
- Edzwald, J. K. *Water Quality & Treatment: A Handbook on Drinking Water*, 6th ed.; McGraw-Hill's AccessEngineering; McGraw-Hill: New York, 2012.
- Graham, M. R.; Summers, R. S.; Simpson, M. R.; Macleod, B. W. Modeling Equilibrium Adsorption of 2-Methylisoborneol and Geosmin in Natural Waters. *Water Research* **2000**, *34* (8), 2291–2300. [https://doi.org/10.1016/S0043-1354\(99\)00390-5](https://doi.org/10.1016/S0043-1354(99)00390-5).
- He, Q.; Lin, Z.; Wang, H.; Zou, Z.; Chen, D.; Yang, K. Odor Removal by Powdered Activated Carbon (PAC) in Low Turbidity Drinking Water. *Water Science & Technology* **2016**, *16* (4), 1017–1023. <https://doi.org/10.2166/ws.2016.017>.
- Hepplewhite, C.; Newcombe, G.; Knappe, D. NOM and MIB, Who Wins in the Competition for Activated Carbon Adsorption Sites? **2004**, *49* (9), 257–265. <https://doi.org/10.2166/wst.2004.0584>.
- International Humic Substances Society, “What are Humic Substances?” <http://humic-substances.org/> (accessed Apr 6, 2020).
- Jaman, S.; Rodriguez, R.; Mazyck, D. Evaluation of Common Granular Activated Carbon Parameters for Trace Contaminant Removal. *Journal of Environmental Engineering* **2019**, *145* (7). [https://doi.org/10.1061/\(ASCE\)EE.1943-7870.0001518](https://doi.org/10.1061/(ASCE)EE.1943-7870.0001518).
- Jüttner, F.; Watson, S. B. Biochemical and Ecological Control of Geosmin and 2-Methylisoborneol in Source Waters. *Appl. Environ. Microbiol.* **2007**, *73* (14), 4395–4406. <https://doi.org/10.1128/AEM.02250-06>.
- Li, Q.; Snoeyink, V. L.; Mariñas, B. J.; Campos, C. Elucidating Competitive Adsorption Mechanisms of Atrazine and NOM Using Model Compounds. *Water Research* **2003**, *37* (4), 773–784. [https://doi.org/10.1016/S0043-1354\(02\)00390-1](https://doi.org/10.1016/S0043-1354(02)00390-1).
- Liato, V.; Aider, M. Geosmin as a Source of the Earthy-Musty Smell in Fruits, Vegetables and Water: Origins, Impact on Foods and Water, and Review of the Removing Techniques. *Chemosphere* **2017**, *181*, 9–18. <https://doi.org/10.1016/j.chemosphere.2017.04.039>.
- Marsh, H; Rodriguez-Reinoso, F. *Activated Carbon*, 1st ed.; Elsevier: Amsterdam, **2006**.
- Mailler, R.; Gasperi, J.; Coquet, Y.; Derome, C.; Buleté, A.; Vulliet, E.; Bressy, A.; Varrault, G.; Chebbo, G.; Rocher, V. Removal of Emerging Micropollutants from Wastewater by Activated Carbon Adsorption: Experimental Study of Different Activated Carbons

- and Factors Influencing the Adsorption of Micropollutants in Wastewater. *Journal of Environmental Chemical Engineering* **2016**, 4 (1), 1102–1109. <https://doi.org/10.1016/j.jece.2016.01.018>.
- Matsui, Y.; Nakao, S.; Yoshida, T.; Taniguchi, T.; Matsushita, T. Natural Organic Matter That Penetrates or Does Not Penetrate Activated Carbon and Competes or Does Not Compete with Geosmin. *Separation and Purification Technology* **2013**, 113 (C), 75–82. <https://doi.org/10.1016/j.seppur.2013.04.009>.
- Matsui, Y.; Yoshida, T.; Nakao, S.; Knappe, D. R. U.; Matsushita, T. Characteristics of Competitive Adsorption between 2-Methylisoborneol and Natural Organic Matter on Superfine and Conventionally Sized Powdered Activated Carbons. *Water Research* **2012**, 46 (15), 4741–4749. <https://doi.org/10.1016/j.watres.2012.06.002>.
- Matsui, Y.; Yoshida, T.; Nakao, S.; Knappe, D. R. U.; Matsushita, T. Characteristics of Competitive Adsorption between 2-Methylisoborneol and Natural Organic Matter on Superfine and Conventionally Sized Powdered Activated Carbons. *Water Research* **2012**, 46 (15), 4741–4749. <https://doi.org/10.1016/j.watres.2012.06.002>.
- Mccallum, R.; Roddick, F.; Hobday, M. Adsorption of MIB by Activated Carbons Produced Using Several Activation Techniques. **2002**, 2 (5–6), 265–270. <https://doi.org/10.2166/ws.2002.0178>.
- Newcombe, G.; Morrison, J.; Hepplewhite, C.; Knappe, D. R. U. Simultaneous Adsorption of MIB and NOM onto Activated Carbon: II. Competitive Effects. *Carbon* **2002**, 40 (12), 2147–2156. [https://doi.org/10.1016/S0008-6223\(02\)00098-2](https://doi.org/10.1016/S0008-6223(02)00098-2).
- Newcombe, G.; Morrison, J.; Hepplewhite, C. Simultaneous Adsorption of MIB and NOM onto Activated Carbon. I. Characterisation of the System and NOM Adsorption. *Carbon* **2002**, 40 (12), 2135–2146. [https://doi.org/10.1016/S0008-6223\(02\)00097-0](https://doi.org/10.1016/S0008-6223(02)00097-0).
- Newcombe, G.; Cook, D. Influences on the Removal of Tastes and Odours by PAC. *Journal of Water Supply : Research and Technology - AQUA* **2002**, 51 (8), 463–474. <https://doi.org/10.2166/aqua.2002.0040>.
- Nowack, K. O.; Cannon, F. S.; Mazyck, D. W. Enhancing Activated Carbon Adsorption of 2-Methylisoborneol: Methane and Steam Treatments. *Environmental science & technology* **2004**, 38 (1), 276–284. <https://doi.org/10.1021/es026397j>.
- Pelekani, C.; Snoeyink, V. L. Competitive Adsorption in Natural Water: Role of Activated Carbon Pore Size. *Water Research* **1999**, 33 (5), 1209–1219. [https://doi.org/10.1016/S0043-1354\(98\)00329-7](https://doi.org/10.1016/S0043-1354(98)00329-7).
- Qi, S.; Schideman, L.; Mariñas, B. J.; Snoeyink, V. L.; Campos, C. Simplification of the IAST for Activated Carbon Adsorption of Trace Organic Compounds from Natural Water. *Water Research* **2007**, 41 (2), 440–448. <https://doi.org/10.1016/j.watres.2006.10.018>.
- Rangel-Mendez, J. R.; Cannon, F. S. Improved Activated Carbon by Thermal Treatment in Methane and Steam: Physicochemical Influences on MIB Sorption Capacity. *Carbon* **2005**, 43 (3), 467–479. <https://doi.org/10.1016/j.carbon.2004.09.031>.

- Rescorla, A.; Semmens, M. J.; Hozalski, R. M. Effect of NOM and Lime Softening on Geosmin Removal by PAC. *Journal - American Water Works Association* **2017**, *109* (4), 15–26. <https://doi.org/10.5942/jawwa.2017.109.0030>.
- Seckler, S.; Margarida, M.; Rosemeire, A. L.; Filho, F. Interference of Iron as a Coagulant on MIB Removal by Powdered Activated Carbon Adsorption for Low Turbidity Waters. *Journal of Environmental Sciences* **2013**, *25* (8), 1575–1582. [https://doi.org/10.1016/S1001-0742\(12\)60231-9](https://doi.org/10.1016/S1001-0742(12)60231-9).
- Shimabuku, K.; Cho, H.; Townsend, E.; Rosario-Ortiz, F.; Summers, R. Modeling Nonequilibrium Adsorption of MIB and Sulfamethoxazole by Powdered Activated Carbon and the Role of Dissolved Organic Matter Competition. *Environmental Science & Technology* **2014**, *48* (23), 13735–13742. <https://doi.org/10.1021/es503512v>.
- Srinivasan, R.; Sorial, G. A. Treatment of Taste and Odor Causing Compounds 2-Methyl Isoborneol and Geosmin in Drinking Water: A Critical Review. *Journal of Environmental Sciences* **2011**, *23* (1), 1–13. [https://doi.org/10.1016/S1001-0742\(10\)60367-1](https://doi.org/10.1016/S1001-0742(10)60367-1).
- Tennant, M. F.; Mazyck, D. W. The Role of Surface Acidity and Pore Size Distribution in the Adsorption of 2-Methylisoborneol via Powdered Activated Carbon. *Carbon* **2007**, *45* (4), 858–864. <https://doi.org/10.1016/j.carbon.2006.11.009>.
- Thermal Analysis Laboratory | Western Kentucky University [https://www.wku.edu/artp/ta\\_lab.php](https://www.wku.edu/artp/ta_lab.php) (accessed Mar 18, 2021).
- US EPA, O. Water Topics <https://www.epa.gov/environmental-topics/water-topics> (accessed Feb 22, 2021).
- Watson, S.; Ridal, J.; Boyer, G. Taste and Odour and Cyanobacterial Toxins: Impairment, Prediction, and Management in the Great Lakes. *Canadian Journal of Fisheries and Aquatic Sciences/Journal Canadien des Sciences Halieutiques et Aquatiques* **2008**, *65* (08), 1779–1796.
- Watson, S. B.; Monis, P.; Baker, P.; Giglio, S. Biochemistry and Genetics of Taste- and Odor-Producing Cyanobacteria. *Harmful Algae* **2016**, *54*, 112–127. <https://doi.org/10.1016/j.hal.2015.11.008>.
- Worch, E. Competitive Adsorption of Micropollutants and NOM onto Activated Carbon: Comparison of Different Model Approaches. *Journal of Water Supply : Research and Technology - AQUA* **2010**, *59* (5), 285–297. <http://dx.doi.org.mines.idm.oclc.org/10.2166/aqua.2010.065>.
- Yuhas, D. Storm Scents: It's True, You Can Smell Oncoming Summer Rain <https://www.scientificamerican.com/article/storm-scents-smell-rain/> (accessed Feb 28, 2021).
- Yu, J.; Yang, M.; Lin, T.-F.; Guo, Z.; Zhang, Y.; Gu, J.; Zhang, S. Effects of Surface Characteristics of Activated Carbon on the Adsorption of 2-Methylisobornel (MIB) and Geosmin from Natural Water. *Separation and Purification Technology* **2007**, *56* (3), 363–370. <https://doi.org/10.1016/j.seppur.2007.01.039>.

- Zhao, Y. H.; Abraham, M. H.; Zissimos, A. M. Fast Calculation of van Der Waals Volume as a Sum of Atomic and Bond Contributions and Its Application to Drug Compounds. *J Org Chem* **2003**, *68* (19), 7368–7373. <https://doi.org/10.1021/jo034808o>.
- Zoschke, K.; Engel, C.; Börnick, H.; Worch, E. Adsorption of Geosmin and 2-Methylisoborneol onto Powdered Activated Carbon at Non-Equilibrium Conditions: Influence of NOM and Process Modelling. *Water Research* **2011**, *45* (15), 4544–4550. <https://doi.org/10.1016/j.watres.2011.06.006>.

APPENDIX A  
SUPPLEMENTARY PAC CHARACTERIZATION DATA

Table A.1 Temperature programmed desorption of surface oxygen functional groups from carbon surface. Water desorbed at room temperature originates from external moisture while that desorbing at higher temperature originates from internal or chemisorbed moisture. CO<sub>2</sub> primarily originates from carboxylic acid groups while CO originates primarily from phenolic hydroxyl groups or quinone carbonyl functionalities.

Temperature	CP500	CPH	CP800F	evolved gas
25°C	0.4	0.6	1.4	H <sub>2</sub> O
25 - 300°C	1.8	1.7	1.9	H <sub>2</sub> O
300 - 400°C	0.3	0.3	0.4	CO <sub>2</sub>
400 - 750°C	1.0	1.3	3.3	CO <sub>2</sub> and CO
750 - 900°C	1.7	1.7	2.1	CO <sub>2</sub> and CO
total 300 - 900°C	3.0	3.3	5.9	-
total	5.3	5.7	9.2	-

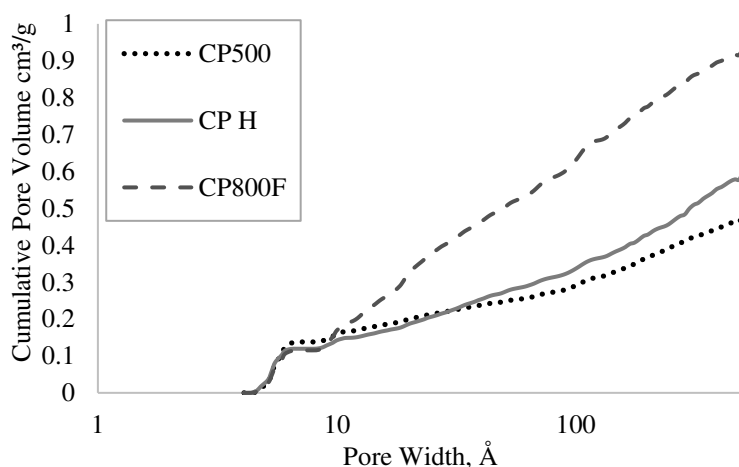


Figure A.1 Cumulative pore volume up to 500 angstroms in cm<sup>3</sup> per gram measured by nitrogen adsorption and modeled the density functional theory.

## APPENDIX B

### ADDITIONAL WATER QUALITY INFORMATION

Table B.1 Summary of inorganic content of Source A and B waters as determined by ICP.

Water	Ca (mg/L)	Na (mg/L)	Mg (mg/L)	K (mg/L)	S (mg/L)
Source A	26.64	14.21	10.74	4.49	22.01
Source B	20.58	7.18	17	2.19	8.35

APPENDIX C

FREUNDLICH ADSORPTION ISOTHERMS

Table C.1 CP500 Freundlich parameters for MIB and GSM adsorption determined in NOM-free water, synthetic waters, and source waters.

Water	Initial DOC (ppm)	MIB - Freundlich Parameters			GSM - Freundlich Parameters		
		1/n	K <sub>f</sub>	R <sub>2</sub>	1/n	K <sub>f</sub>	R <sub>2</sub>
NOM-free (HPLC)	0.0	0.14	4.18	0.58	0.25	3.34	0.95
SWR NOM	3.2	0.11	0.95	0.46	0.25	1.18	0.97
	6.6	0.31	0.27	0.91	0.33	0.58	0.97
	8.9	0.24	0.34	0.92	0.29	0.71	0.95
UM NOM	3.2	0.15	0.70	0.93	0.28	0.88	0.97
	6.1	0.15	0.52	1.00	0.31	0.66	0.89
	8.9	0.20	0.36	0.84	0.33	0.53	0.99
SWR HA	3.1	0.36	0.73	1.00	0.37	1.17	0.99
	6.1	0.32	0.57	0.99	0.38	0.94	0.96
	9.1	0.27	0.52	0.76	0.36	0.73	0.97
SWR FA	3.3	0.42	0.34	1.00	0.41	0.81	1.00
	6.3	0.27	0.36	0.92	0.35	0.69	0.95
	9.3	0.35	0.29	0.99	0.37	0.65	0.98
Source A	12.2	0.26	0.24	0.84	0.32	0.42	0.96
	9.3	0.21	0.30	0.86	0.32	0.48	0.95
	6.3	0.28	0.32	0.94	0.34	0.62	0.95
	3.3	0.28	0.44	0.89	0.32	0.91	0.94
Source B	6.3	0.32	0.29	1.00	0.39	0.47	0.98
	5.0	0.36	0.36	0.99	0.39	0.67	1.00
	3.7	0.43	0.33	0.99	0.41	0.71	0.99
	2.1	0.34	0.58	0.96	0.37	0.95	0.98
Source C	3.9	0.23	0.42	0.68	0.33	0.74	1.00
Source D	3.1	0.09	0.46	0.40	0.33	0.52	0.98

Table C.2 Freundlich parameters for MIB and GSM adsorption on to CPH determined in NOM-free water, SWR NOM, and source A waters.

Water	Initial DOC (ppm)	MIB - Freundlich Parameters			GSM - Freundlich Parameters		
		1/n	K <sub>f</sub>	R <sub>2</sub>	1/n	K <sub>f</sub>	R <sub>2</sub>
NOM-free (HPLC)	0.0	0.14	5.47	0.71	0.28	4.07	0.80
	3.1	0.41	0.54	0.99	0.37	1.30	0.90
SWR NOM	6.2	0.38	0.50	1.00	0.33	1.24	0.80
	9.3	0.43	0.30	0.92	0.29	1.04	0.88
Source A	3.2	0.35	0.58	0.98	0.22	1.80	0.88
	6.2	0.44	0.32	0.46	0.25	0.95	0.58
	9.3	0.36	0.36	1.00	0.25	0.58	0.49

Table C.3 Freundlich parameters for MIB and GSM adsorption onto CP800F determined in NOM-free water, SWR NOM, and source A waters.

Water	Initial DOC (ppm)	MIB - Freundlich Parameters			GSM - Freundlich Parameters		
		1/n	K <sub>f</sub>	R <sub>2</sub>	1/n	K <sub>f</sub>	R <sub>2</sub>
NOM-free (HPLC)	0.0	0.18	5.36	0.95	0.38	3.99	0.98
	3.1	0.62	0.39	0.99	0.49	1.34	0.92
SWR NOM	6.2	0.38	0.65	0.98	0.48	1.10	0.89
	9.3	0.48	0.36	1.00	0.46	1.02	0.94
Source A	3.2	0.59	0.33	0.80	0.46	1.17	1.00
	6.2	0.45	0.38	0.98	0.40	0.94	0.99
	9.3	0.29	0.55	0.94	0.43	0.53	1.00



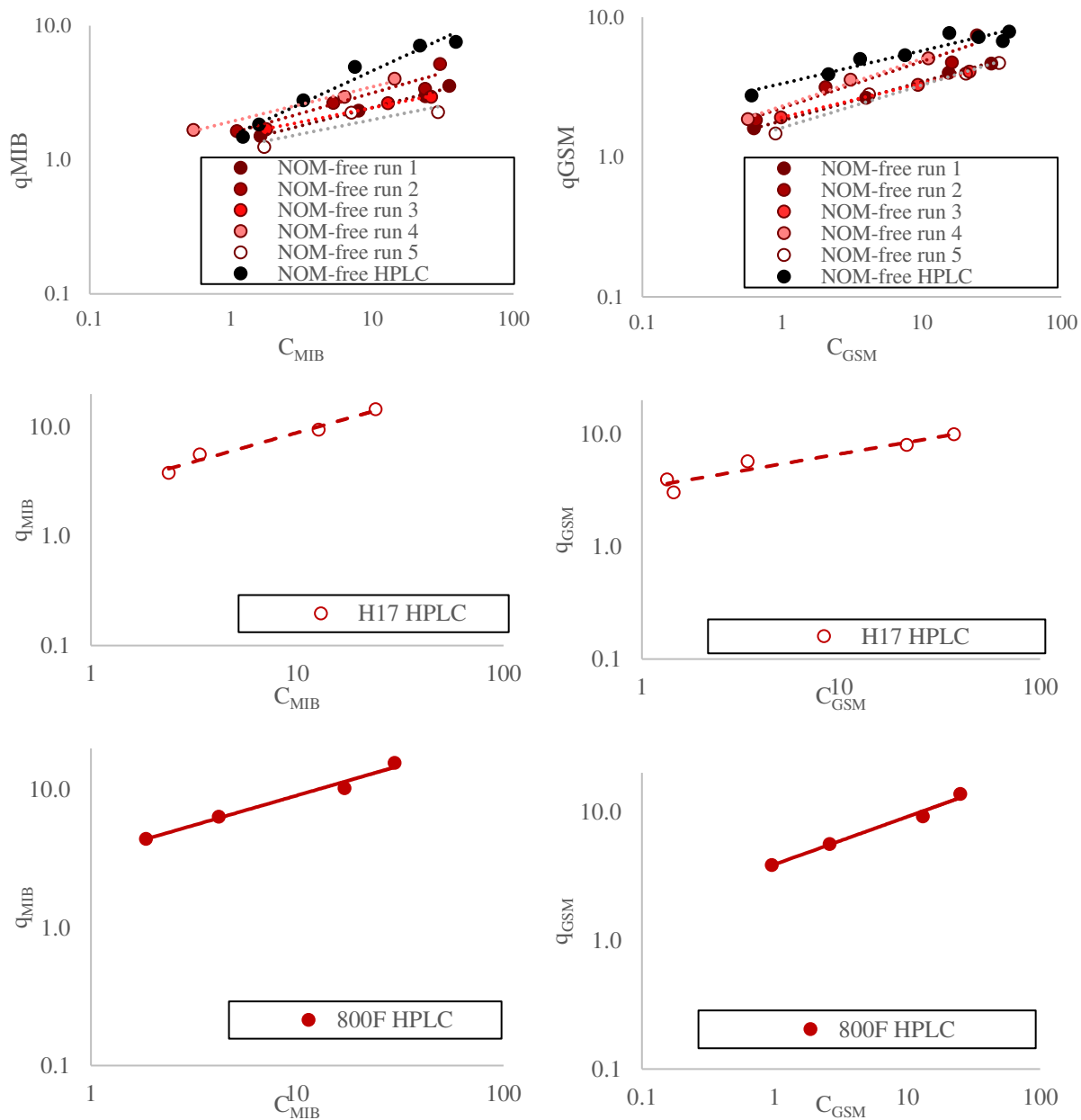


Figure C.1 Non-equilibrium adsorption isotherms for MIB and GSM onto CP500 (top) CPH (middle) CP800F (bottom) in NOM-free waters. Units of  $q_{MIB}$  and  $q_{GSM}$  are in  $\mu\text{g/g}$  and units of  $C_{MIB}$  and  $C_{GSM}$  are in  $\text{ng/L}$ . Trend lines represent Freundlich lines of best fit.

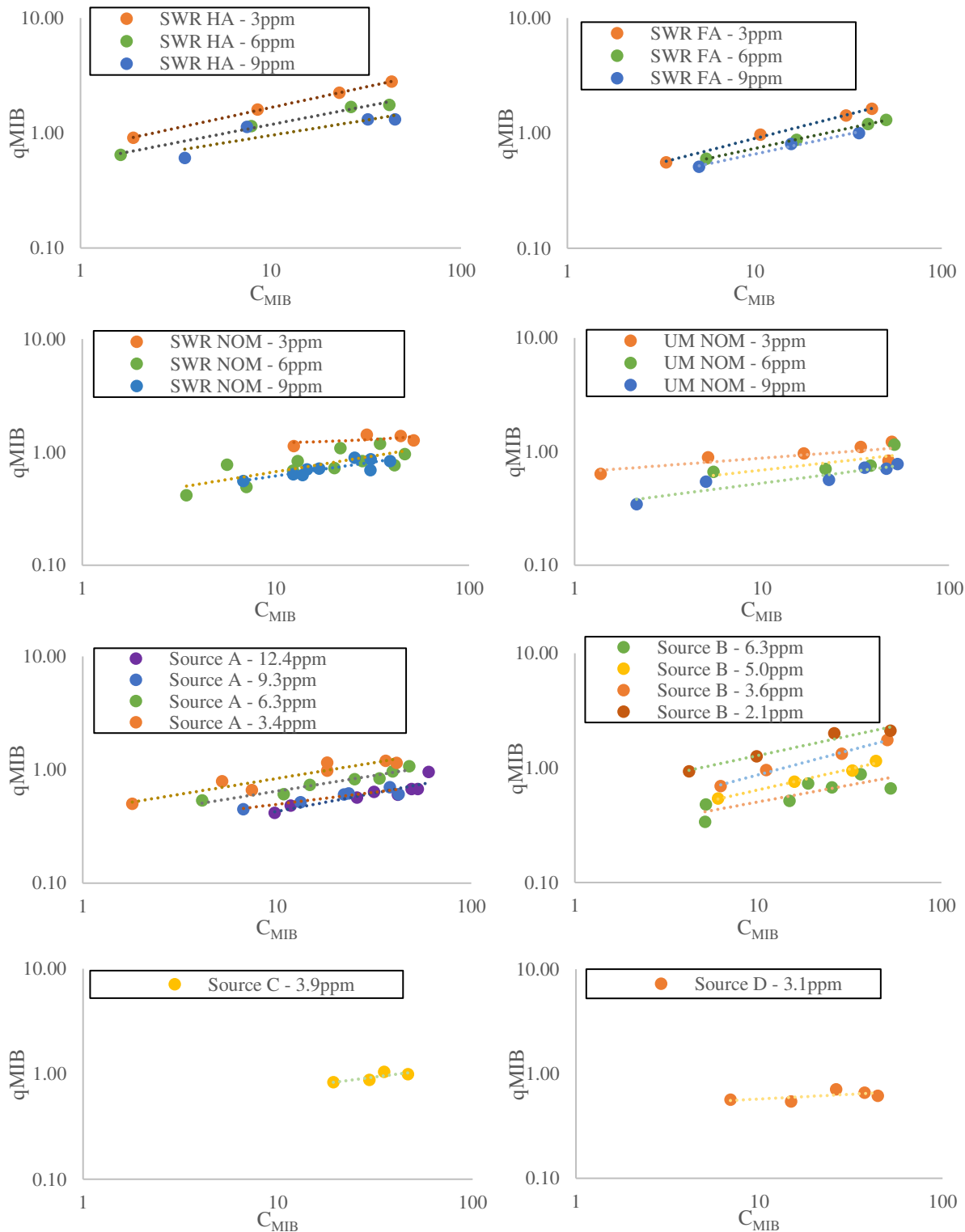


Figure C.2 Non-equilibrium adsorption isotherms for MIB onto CP500 in surface waters and synthetic waters. Units of  $q_{MIB}$  are in  $\mu\text{g/g}$  and units of  $C_{MIB}$  and in  $\text{ng/L}$ . Trend lines represent Freundlich lines of best fit.

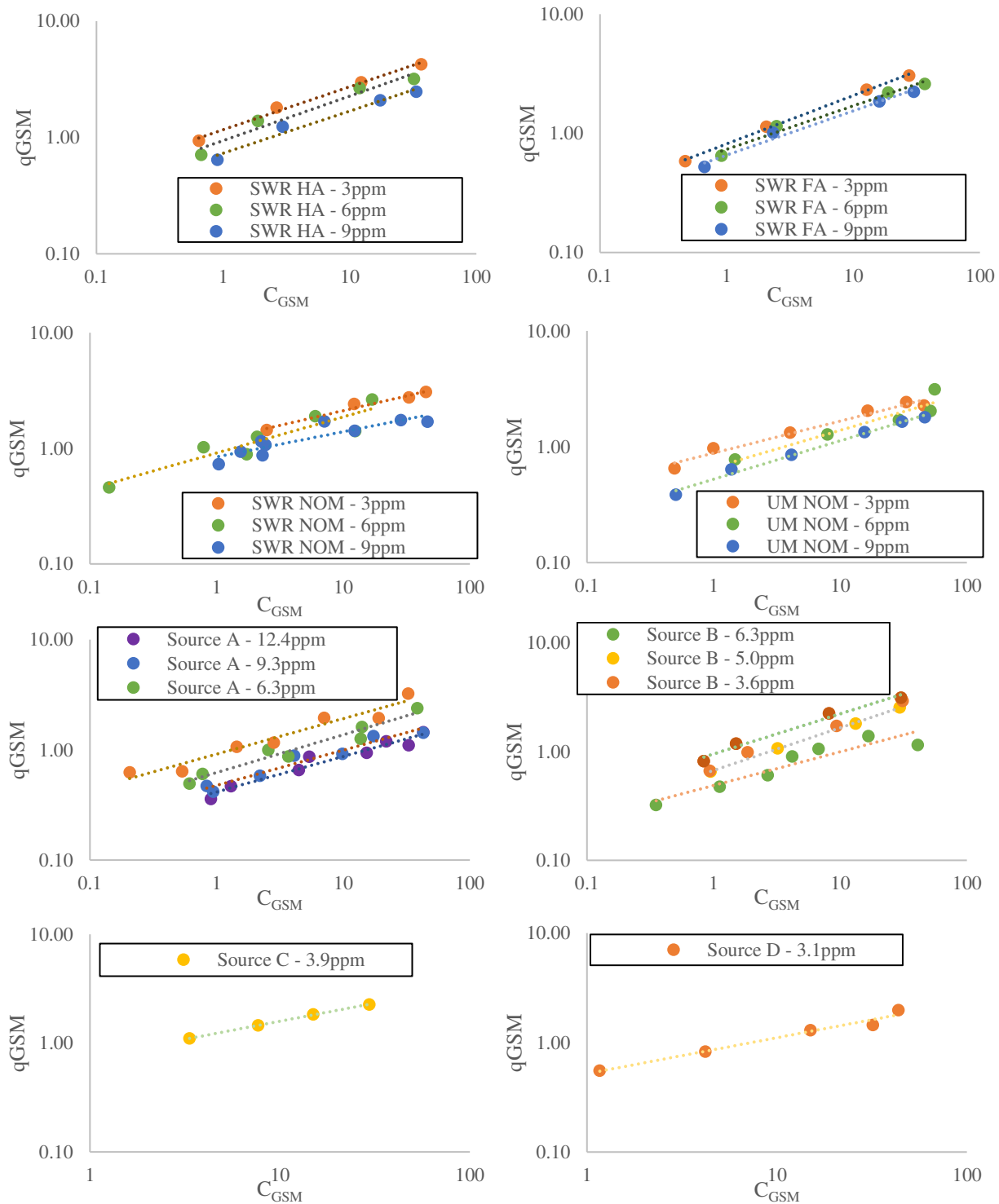


Figure C.3 Non-equilibrium adsorption isotherms for GSM onto CP500 in surface waters and synthetic waters. Units of  $q_{GSM}$  are in  $\mu\text{g/g}$  and units of  $C_{GSM}$  and in  $\text{ng/L}$ . Trend lines represent Freundlich lines of best fit.

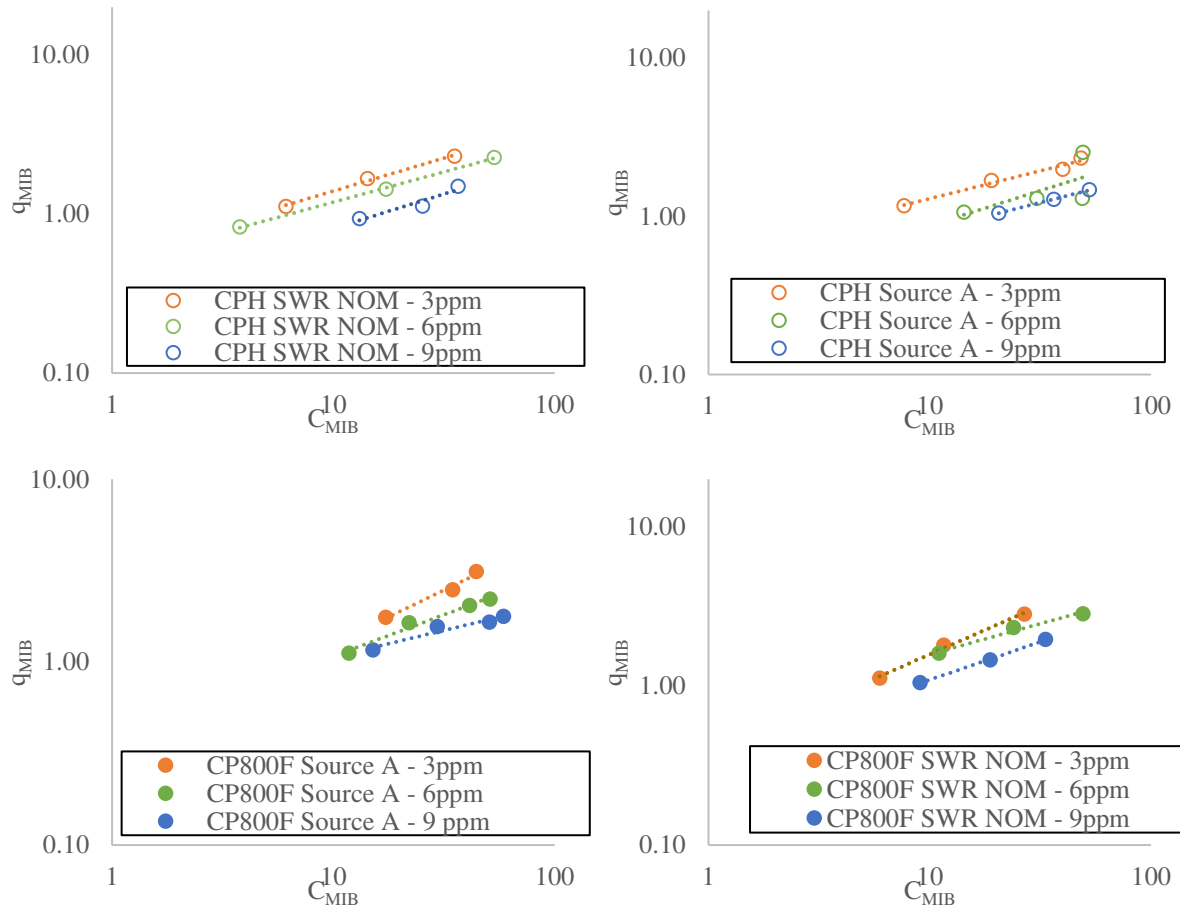


Figure C.4 Non-equilibrium adsorption isotherms for MIB onto CPH and CP800F source A and SWR NOM synthetic water at 3, 6, and 9 ppm DOC. Units of  $q_{MIB}$  are in  $\mu\text{g/g}$  and units of  $C_{MIB}$  and in  $\text{ng/L}$ . Trend lines represent Freundlich lines of best fit.

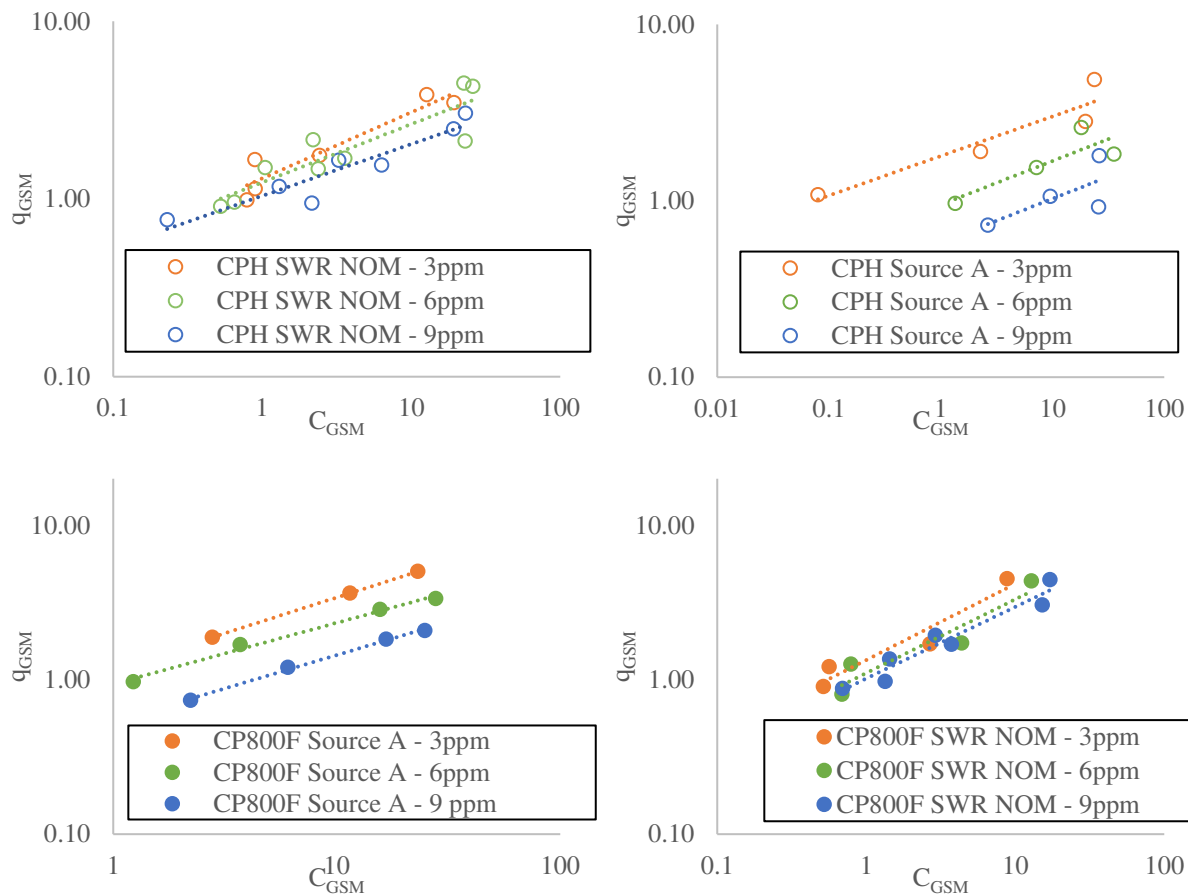


Figure C.5 Non-equilibrium adsorption isotherms for GSM onto CPH and CP800F in source A and SWR NOM synthetic waters at 3, 6, and 9 ppm DOC. Units of  $q_{GSM}$  are in  $\mu\text{g/g}$  and units of  $C_{GSM}$  and in  $\text{ng/L}$ . Trend lines represent Freundlich lines of best fit.

## APPENDIX D

### MIB AND GSM REMOVAL CURVES

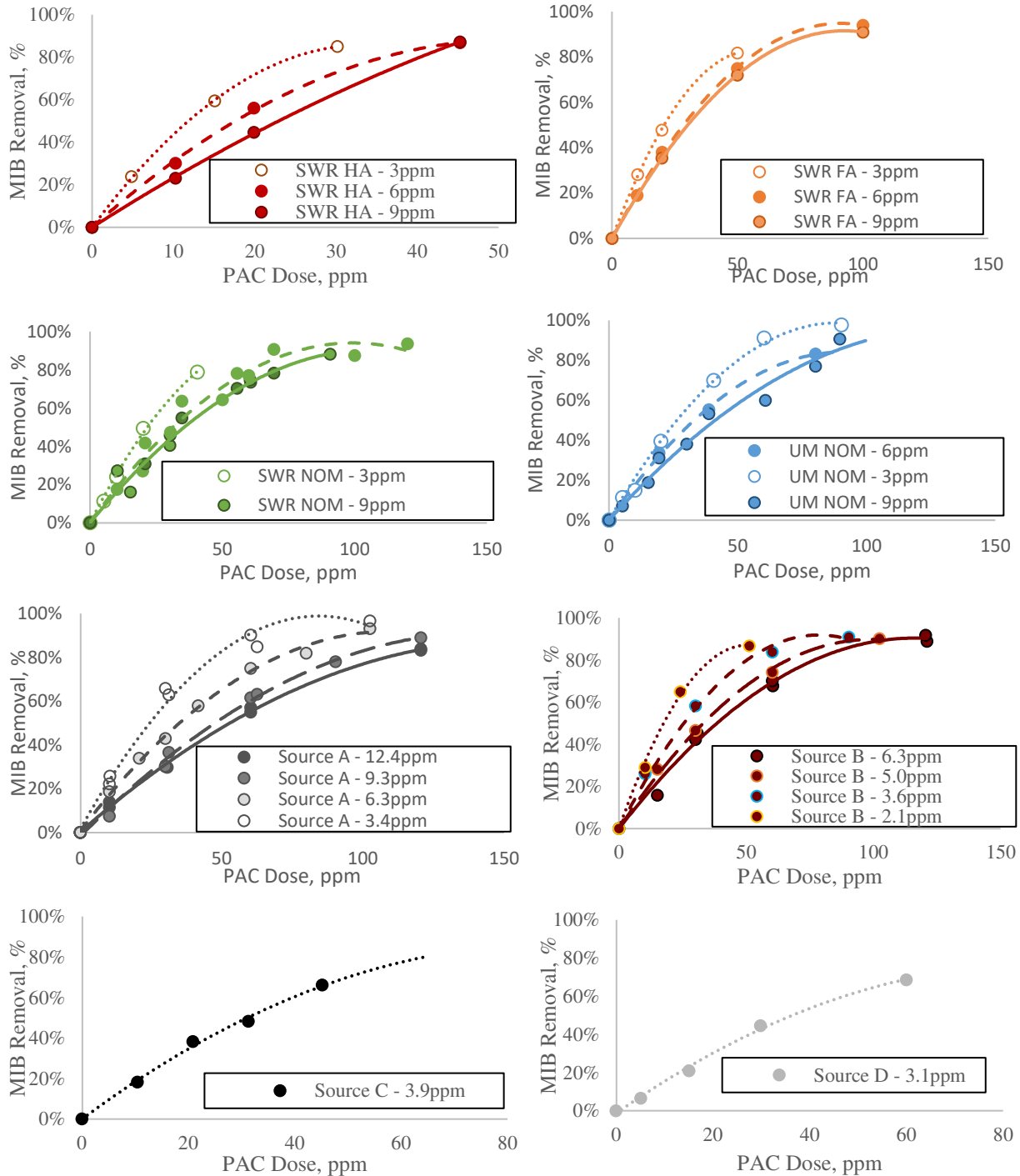


Figure D.1 MIB removal curves for CP500 conducted at 60 ppt MIB and 30-minute contact time in: SWR HA, SWR FA, SWR NOM, UM NOM, source A, source B, and source C.

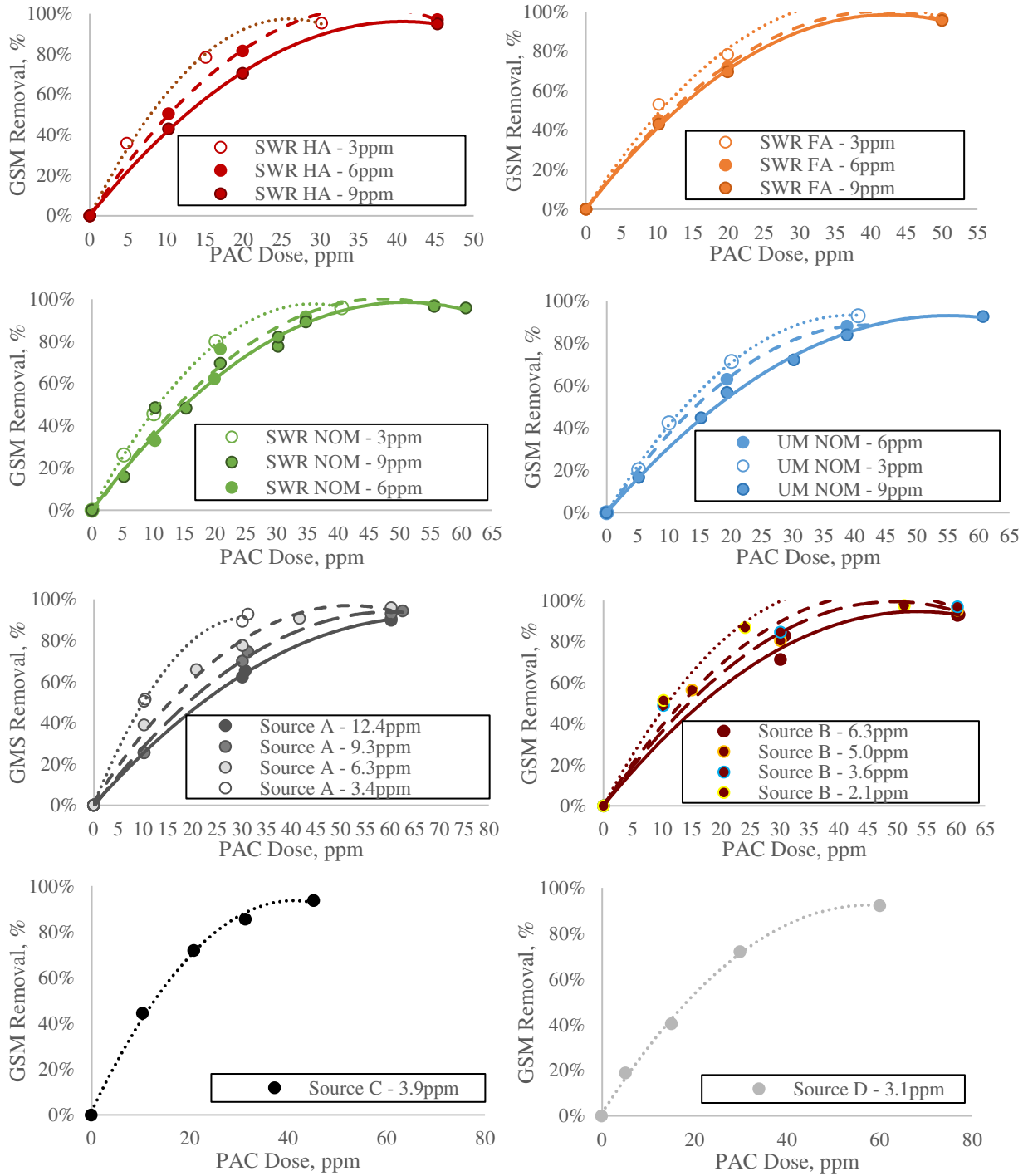


Figure D.2 GSM removal curves for CP500 conducted at 60 ppt GSM and 30-minute contact time in: SWR HA, SWR FA, SWR NOM, UM NOM, source A, source B, and source C.

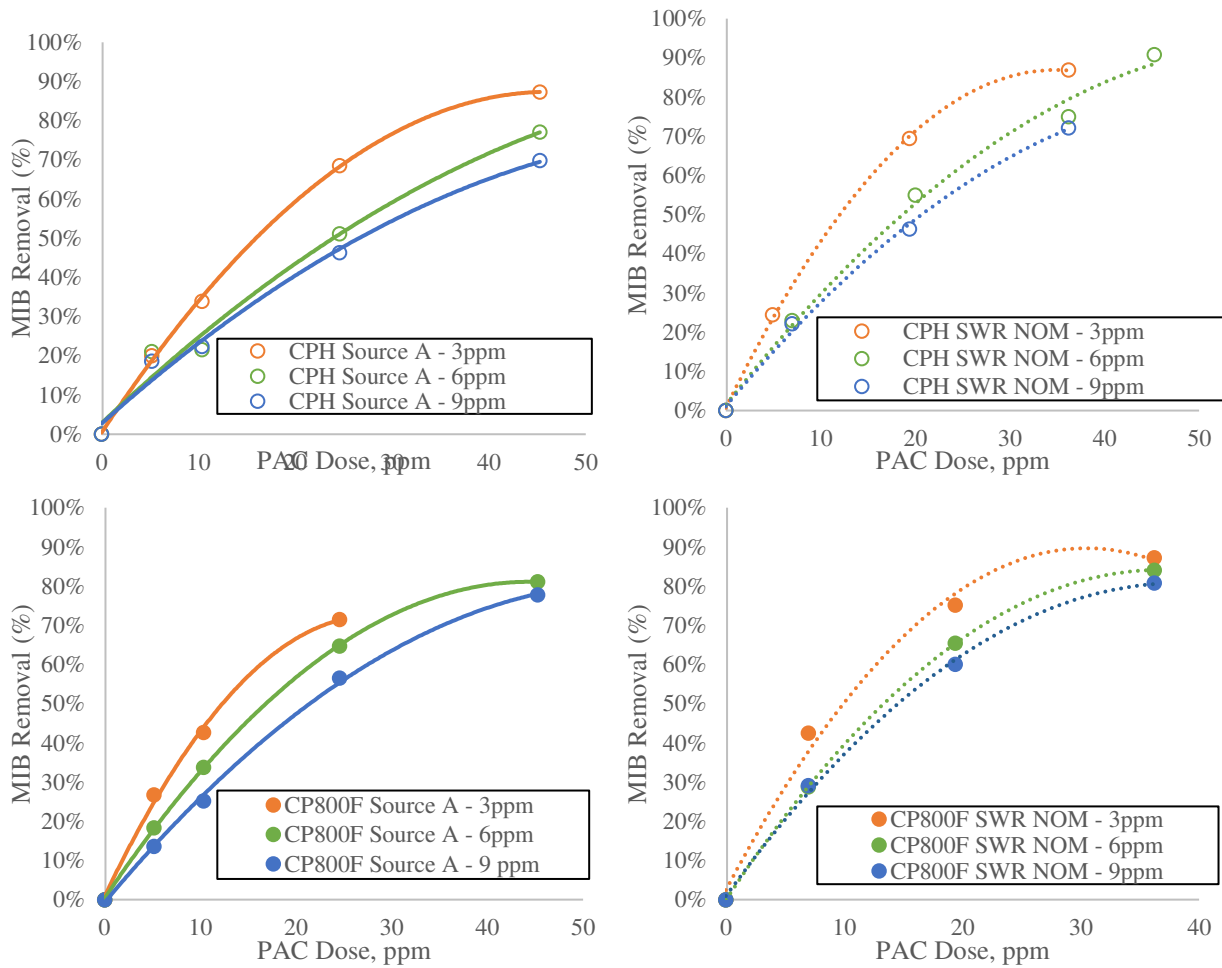


Figure D.3 MIB removal curves for CPH and CP800F conducted at 60 ppt MIB and 30-minute contact time for source A and SWR NOM at 3, 6, and 9 ppm DOC.



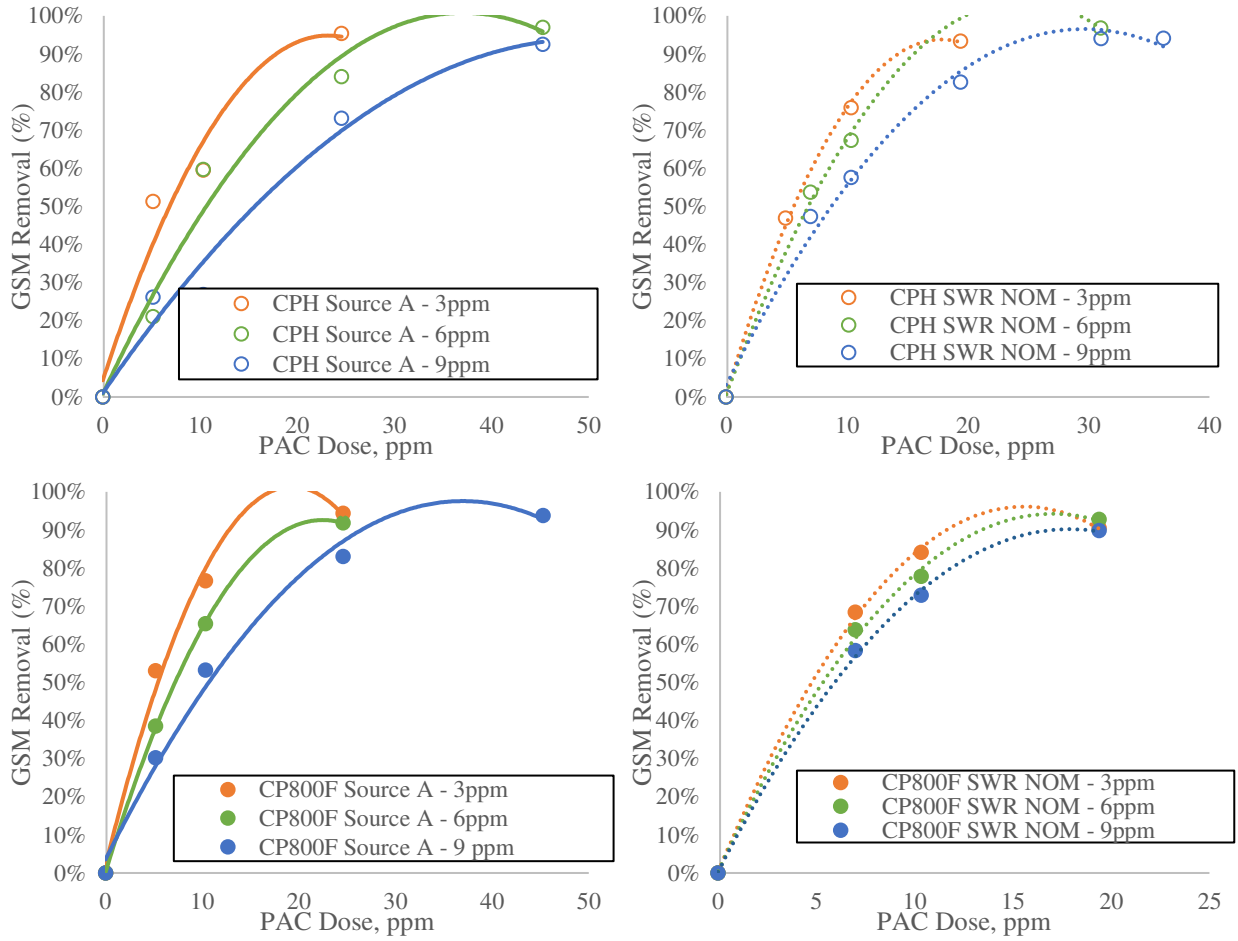


Figure D.4 GSM removal curves for CPH and CP800F conducted at 60 ppt GSM and 30-minute contact time for source A and SWR NOM at 3, 6, and 9 ppm DOC.

APPENDIX E  
DOC REMOVAL CURVES

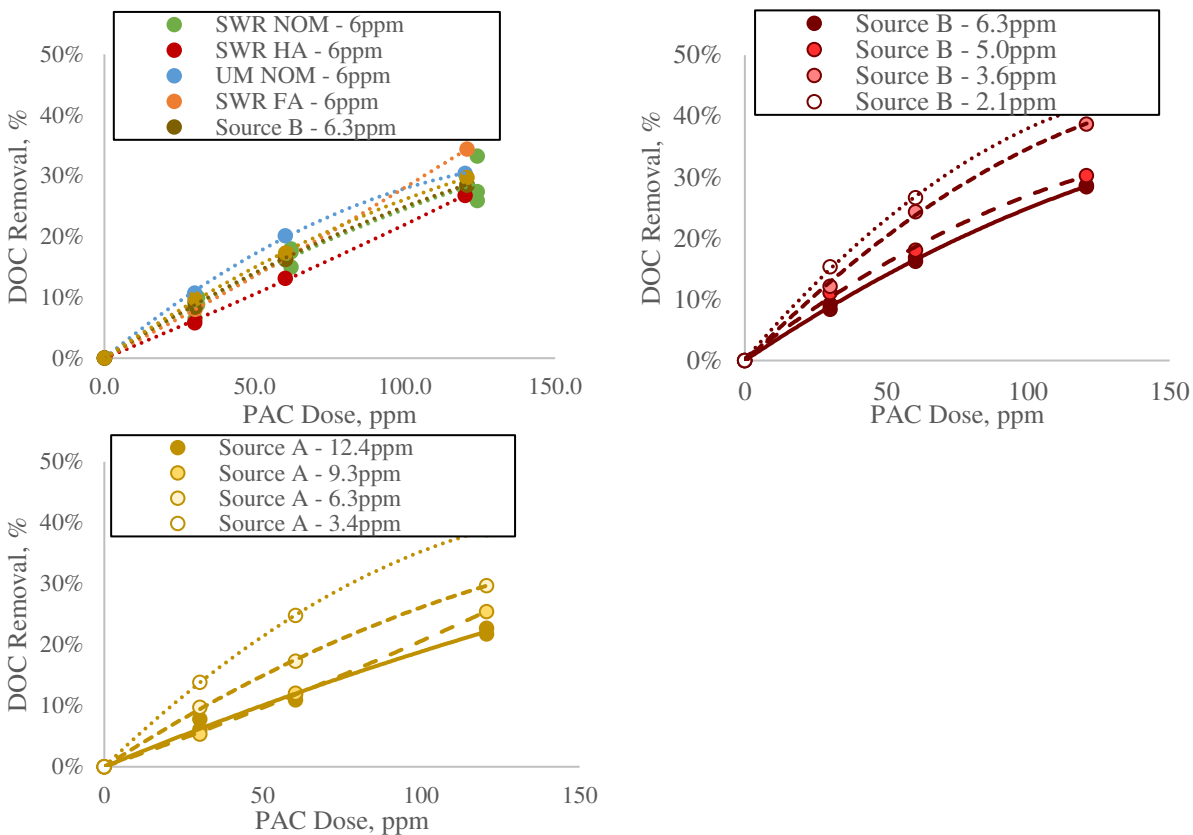


Figure E.1 DOC removal curves using CP500 in synthetic and source waters at various initial DOC concentrations.

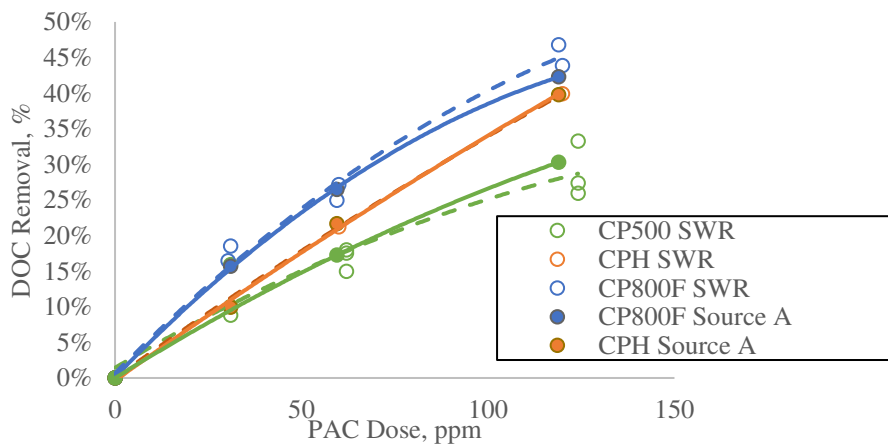


Figure E.2 DOC removal curves using CPH and CP800F in SWR NOM and Source A waters both at 6 ppm DOC initially.